Comprehensive studies of low-spin collective excitations in ^{94}Mo

C. Fransen,[1,2] N. Pietralla,[1] Z. Ammar,[2] D. Bandyopadhyay,[2] N. Boukharouba,[2] P. von Brentano,[1] A. Dewald,[1] J. Gableske,[1] A. Gade,[1,*] J. Jolie,[1] U. Kneissl,[3] S. R. Lesher,[2] A. F. Lisetskiy,[1] M. T. McEllistrem,[2] M. Merrick,[2] H. H. Pitz,[3] N. Warr,[1] V. Werner,[1] and S. W. Yates[2]

[1]*Institut für Kernphysik, Universität zu Köln, D-50937 Köln, Germany*

[2]*Departments of Physics & Astronomy and Chemistry, University of Kentucky, Lexington, Kentucky 40506-0055*

[3]*Institut für Strahlenphysik, Universität Stuttgart, D-70569 Stuttgart, Germany*

(Received 17 September 2002; published 19 February 2003)

Excited low-spin states in ^{94}Mo have been studied extensively with a combination of γ-ray spectroscopic techniques. We have performed photon scattering experiments, $\gamma\gamma$ coincidence measurements following the β^+ decay of ^{94}Tc^m, in-beam $\gamma\gamma$ coincidence studies with the reaction ^{91}Zr$(\alpha,n)^{94}$Mo, and ^{94}Mo$(n,n'\gamma)$ measurements. These experiments yielded detailed information about the low-spin level scheme of ^{94}Mo. From measured lifetimes, branching ratios, and multipole mixing ratios, many absolute transition strengths were determined. These data permitted the interpretation of several low-spin states in terms of collective excitations, that are not fully symmetric with respect to the proton-neutron degree of freedom, the so-called mixed-symmetry (MS) states: The one-phonon 2^+ MS state and three members of an expected multiplet of two-phonon MS states were identified from absolute $M1$ and $E2$ transition strengths. The data also enable us to identify several proton-neutron-symmetric multiphonon states.

DOI: 10.1103/PhysRevC.67.024307 PACS number(s): 21.10.Re, 21.10.Tg, 25.20.Dc, 27.60.+j

I. INTRODUCTION

The nuclide ^{94}Mo is formed by $Z=42$ protons and $N=52$ neutrons. With the small number of only two valence neutrons outside the $N=50$ neutron shell closure, this nucleus is expected to exhibit the properties of a quantum vibrator. This fact makes ^{94}Mo a good subject of a detailed search for low-lying collective vibrational excitations.

^{94}Mo has very recently attracted a great deal of attention because some of its low-spin off-yrast states were identified, from a comprehensive data set on electromagnetic transition strengths, as forming a quadrupole-collective multiphonon structure with mixed proton-neutron symmetry [1–3]. These findings have initiated theoretical investigations [4–7] of the low-spin structure of ^{94}Mo and an experimental research effort on $N=52$ isotones [8,9]. In this paper, we offer a comprehensive presentation of our data on ^{94}Mo.

The phonon scheme is a simple but useful concept in nuclear structure physics [10]. The lowest collective $J^\pi=2^+$ and 3^- states in nearly spherical nuclei can be considered as quadrupole and octupole vibrations, which represent the most important vibrational degrees of freedom at low energies. Multiphonon states can result from the coupling of collective excitations. For example, multi-quadrupole-phonon states and double-octupole states have been studied a lot (see, e.g., [11,12]). Interesting is the case of inhomogeneous phonon coupling [13] where different vibrational quanta may couple. Particularly pure multiphonon states can be expected for this case because anharmonicities due to the effects of the Pauli principle in the formation of the multiphonon wave functions must be expected to be small. The best studied example for inhomogeneous phonon coupling is the quadrupole-octupole coupling [14]. A $J^\pi=1^-$ two-phonon state with the structure $(2^+\otimes 3^-)1^-$ has been studied systematically in heavy nuclei; see, e.g., [15,16] and references therein.

Another important class of nuclear excitations, which are fundamental for the understanding of nuclear structure, is represented by collective states that are not symmetric with respect to the proton-neutron (pn) degree of freedom. These states were predicted in the pn version of the interacting boson model (IBM-2) [17–20], and their properties were summarized in Ref. [21]. These pn nonsymmetric states decay by strong $M1$ transitions and act in the IBM as building blocks of nuclear structures even capable of forming multiphonon excitations in vibrational nuclei. Similar multiphonon states built on an isovector quadrupole excitation were predicted for vibrators in the 1960s [22], but at much higher excitation energies than later observed.

In the IBM-2, states can be classified using the F-spin quantum number [17,19], which is for elementary proton and neutron bosons the analogue of the isospin quantum number for nucleons. The IBM-2 wave functions with $F=F_{\max}=N/2$ represent symmetric states, as they are symmetric under the pairwise exchange of proton and neutron labels. $N_B=N_\pi+N_\nu$ here denotes the total number of proton and neutron bosons. Excited states with $F<F_{\max}$, on the other hand, contain at least one pair of proton and neutron bosons which is antisymmetric under the exchange of nucleon labels; thus these states are called mixed-symmetry (MS) states. In this paper we will restrict our discussion to MS states with an F-spin quantum number $F=F_{\max}-1$. The next family is expected at much higher excitation energies.

The IBM-2 predicts distinct signatures for MS states which are accessible to γ-ray spectroscopy: a low excitation energy, weakly collective, F-vector $E2$ transitions to symmetric states, and strong $M1$ transitions to (some) symmetric states with matrix elements of about

*Present address: NSCL, Michigan State University, East Lansing, Michigan 48824-1321.

$$|\langle J^f_{\rm sym}\|M1\|J^i_{\rm ms}\rangle| \approx 1\,\mu_N. \quad (1)$$

In the recently proposed Q-phonon scheme [23–26], which is an approximate scheme in the IBM, the lowest symmetric and MS states [27] can be approximated by simple expressions with the proton and neutron boson quadrupole operators (Q_π, Q_ν) coupled to the symmetric Q phonon, $Q_{\rm s}=Q_\pi+Q_\nu$, and the MS Q phonon, $Q_{\rm m}=Q_\pi/N_\pi - Q_\nu/N_\nu$ [1];

$$|2^+_1\rangle \propto Q_{\rm s}|0^+_1\rangle, \quad (2)$$

$$|J^+_{\rm s}\rangle \propto (Q_{\rm s}Q_{\rm s})^{(J)}|0^+_1\rangle \quad \text{with} \quad J=0,2,4, \quad (3)$$

$$|2^+_{1,\rm ms}\rangle \propto Q_{\rm m}|0^+_1\rangle, \quad (4)$$

$$|L^+_{\rm s}\rangle \propto (Q_{\rm s}Q_{\rm m})^{(L)}|0^+_1\rangle \quad \text{with} \quad L=0,1,2,3,4. \quad (5)$$

As one can see from Eq. (4) the one-Q-phonon 2^+ MS state is the fundamental MS excitation and is orthogonal to the symmetric 2^+_1 state. Moreover, we expect the existence of a full multiplet of two-Q-phonon MS states resulting from the coupling of $Q_{\rm s}$ and $Q_{\rm m}$, with spin quantum numbers 0, 1, 2, 3, and 4, if the Hamiltonian describes a pure vibrator, and if $N_B>2$.

From the measurement of absolute transition strengths, $2^+_{1,\rm ms}$ states have been identified in several weakly deformed nuclei [28–32]. Recently, the $2^+_{1,\rm ms}$ state was identified in the $N=52$ nucleus ^{96}Ru at an excitation energy of 2283.8 keV [8,9].

The 1^+ member of the two-Q-phonon multiplet of MS states ($1^+_{\rm ms}$) is frequently called the ''scissors mode'' due to its geometrical picture in rotational nuclei. It was predicted by Lo Iudice and Palumbo [33] in the two-rotor model. The scissors mode was discovered by Richter in electron scattering experiments in the early 1980s [34]. Since that time, this excitation has been systematically investigated in heavy nuclei in (e,e') [35] and photon scattering studies [36]. Systematic studies of the $M1$ excitation strength [37,38] and the excitation energy of the scissors mode [26,39] have yielded considerable knowledge about this excitation, mostly in the rare earth region.

Less is known about the other MS states. After their recent discovery in ^{94}Mo, candidates for 2^+ and 3^+ two-Q-phonon MS states were found in the $N=52$ isotone ^{96}Ru from $E2/M1$ mixing ratios, branching ratios, and upper lifetime limits [9]. In experiments on ^{142}Ce and ^{144}Nd with inelastic neutron scattering [40,41], 3^+ states, which may represent fragments of a two-Q-phonon 3^+ MS excitation, were strongly suggested, but no clear identification was possible. From experiments on nuclei in the $A=100$ mass region, MS character was tentatively assigned to states with $J>2$ from the measurement of $E2/M1$ mixing ratios (see, e.g., [42]), but because no lifetimes were obtained in these experiments, no transition strengths were determined, preventing a clear identification of the MS character.

Special attention was paid to the identification of multiphonon structures, in particular those with MS character, i.e., the one-Q-phonon $2^+_{1,\rm ms}$ state and the two-Q-phonon multiplet of MS states. The most important results, namely the identification of the fundamental $2^+_{1,\rm ms}$ state and the 1^+, 2^+, and 3^+ members of the two-Q-phonon MS multiplet in ^{94}Mo have been published recently [1–3].

We performed experiments on ^{94}Mo at the Cologne TANDEM accelerator using the β^+ decay of ^{94}Tc$^{\rm m}$ to ^{94}Mo, whereas ^{94}Tc$^{\rm m}$ was produced with the reaction ^{94}Mo$(p,n)^{94}$Tc$^{\rm m}$, and the fusion-evaporation reaction ^{91}Zr$(\alpha,n)^{94}$Mo in combination with photon scattering experiments at the Stuttgart DYNAMITRON accelerator and neutron scattering experiments at the electrostatic accelerator of the University of Kentucky. These experiments yielded detailed data about the low-spin level scheme of this nucleus. The goals of the new neutron scattering measurements were to verify the lifetimes from the earlier experiments, to measure additional lifetimes, and to search for 0^+ states because there exists only sparse data about 0^+ states in ^{94}Mo.

In Sec. II we describe the experimental methods used to study highly excited low-spin states in ^{94}Mo. In Sec. III we present our experimental results. In Sec. IV we discuss the identification of MS states from our measurements of absolute transition strengths, and in Sec. V we discuss the properties of additional collective excitations.

II. EXPERIMENTAL METHODS AND DATA EVALUATION

Each of the methods employed in this study offers particular advantages. The spectroscopy of resonant scattered photons provides integrated photon scattering cross sections and information about the spin quantum numbers of dipole and quadrupole excitations. The very clean off-beam measurement of $\gamma\gamma$ coincidences of transitions following the β^+ decay of ^{94}Tc$^{\rm m}$ to ^{94}Mo enabled us to observe small γ branches and determine the multipolarities of decay transitions. In the fusion-evaporation reaction ^{91}Zr$(\alpha,n)^{94}$Mo, all medium spin states in a certain spin range up to spin $J=8$ and excitation energy window up to about 4 MeV well above the yrast line are populated. From this experiment we obtained multipolarities and branching ratios of decay transitions and spin quantum numbers and some lifetimes of excited states, using the Doppler shift attenuation method (DSAM) [43]. But, because of the Q value of the ^{91}Zr(α,n) reaction of -5.13 MeV, the maximum excitation energy for ^{94}Mo is $E_{\rm max}=9.87$ MeV for an α beam energy of $E_\alpha=15$ MeV. Therefore, unobserved feeding from higher states takes place and we measured only effective lifetimes in this experiment. To establish more absolute lifetimes and to obtain additional information about the low-spin level scheme of ^{94}Mo, further experiments were performed using the reaction ^{94}Mo$(n,n'\gamma)$ at the electrostatic accelerator of the University of Kentucky.

A. Photon scattering experiments

The photon scattering experiments were performed at the DYNAMITRON accelerator at the Institut für Strahlenphysik of the University of Stuttgart [36]. This accelerator produces a monoenergetic electron beam which is stopped in a gold radiator target to produce a continuous bremsstrahlung spec-

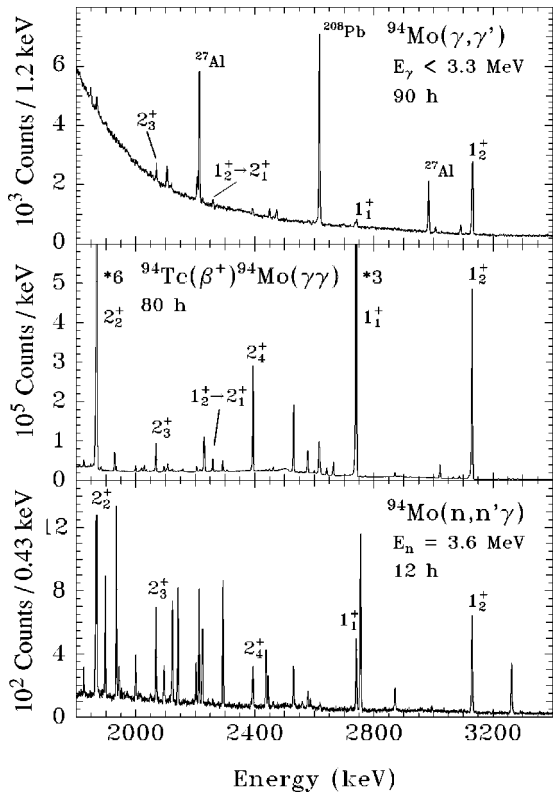

FIG. 1. γ-ray spectra of ^{94}Mo in the energy range from 1.8 to 3.4 MeV. The upper part shows the photon scattering spectrum off ^{94}Mo, the middle part the off-beam γ-ray spectrum following the β^+-decay of ^{94}Tc^m, and the lower part the γ-ray spectrum of the ^{94}Mo$(n,n'\gamma)$ reaction. Ground state transitions are marked with the spins of the corresponding states. At 2067 and 3129 keV we observed ground state transitions of strongly excited 2^+ and 1^+ states, respectively. The lines marked with "^{27}Al" in the photon scattering spectrum arise from the photon flux calibration standard ^{27}Al, which was irradiated simultaneously for calibration purposes.

trum with the incident electron beam energy as the end point energy. Two experiments were performed with the photon scattering technique. A first experiment with an energy of the electron beam of 4.0 MeV served to investigate excited states in the energy region above 3 MeV. In a second experiment, a lower beam energy of 3.3 MeV was used to increase the sensitivity in the energy range around 2 MeV. The target consisted of 0.9997 g of metallic Mo with an enrichment of 93.77 % in ^{94}Mo and 0.4874 g with an enrichment of 77.90 %. In total, the target thickness was 0.840 g/cm^2. For photon flux calibration purposes the target also contained 0.2540 g ^{27}Al, corresponding to a thickness of 0.144 g/cm^2. The scattered γ rays were detected with three high-purity Ge (HPGe) detectors, each with an efficiency of 100 % relative to a 3in.$\times$3in. NaI detector. The detectors were mounted at angles of 90°, 127°, and 150° relative to the beam axis to get information about the spin quantum numbers of excited states by measuring the angular distribution of the scattered γ rays. Figure 1 shows the photon scattering spectrum of ^{94}Mo taken at incident photon energies of $E_\gamma < 3.3$ MeV. A 1^+ state at 3128.3 keV and a 2^+ state at 2067 keV were strongly excited.

We measured the photon scattering cross sections

$$I_{s,f} = g\pi^2 \lambda\!\!\!^{-2} \frac{\Gamma_0 \Gamma_f}{\Gamma}, \tag{6}$$

relative to the well-known cross sections of ^{27}Al [44], which was irradiated simultaneously. $g=(2J+1)/(2J_0+1)$ is a statistical factor, J_0 and J are the ground state spin and the spin of the excited state, and $\lambda\!\!\!^{-}=\hbar c/E_\gamma$ is the reduced wavelength. Γ and Γ_0 (Γ_f) are the total level width and the partial decay width to the ground (final) state, respectively. A detailed description of the photon scattering technique, including the procedure of lifetime determination from the measured photon scattering cross sections, can be found, e.g., in Ref. [36].

B. β-decay experiment

The β-decay experiment was performed at the TANDEM accelerator in Cologne. We produced ^{94}Tc^m nuclei in the center of the Cologne OSIRIS cube coincidence spectrometer using the reaction ^{94}Mo$(p,n)^{94}$Tc^m at a beam energy of $E_p = 13$ MeV. The beam was periodically switched on for 5 s to produce ^{94}Tc^m nuclei and switched off for 5 s to observe γ-ray singles spectra and $\gamma\gamma$ coincidences of transitions following the β^+ decay to ^{94}Mo. ^{94}Tc^m is the $(2)^+$ low-spin isomer of the nuclide ^{94}Tc with a half-life of 52 min and a 7^+ ground state with a half-life of 293 min [45]. The low angular momentum transfer in the ^{94}Mo$(p,n)^{94}$Tc reaction with a beam energy of $E_p = 13$ MeV of about $6\hbar$ favored the population of the $(2)^+$ isomer ^{94}Tc^m, which decays mainly to low-spin states in ^{94}Mo. The middle part of Fig. 1 depicts the off-beam γ-ray singles spectrum of this experiment.

The high counting rate, the low background in this off-beam measurement, and the isotropy of the γ radiation after the β decay enabled us to precisely determine the intensity ratios Γ_f/Γ. From the $\gamma\gamma$ angular correlations we obtained information about the level scheme, multipolarities of transitions, and spins of excited states.

The OSIRIS cube coincidence spectrometer in Cologne was equipped with eight HPGe detectors in this experiment. Six of them were equipped with Compton suppression shields. Two detectors were mounted at a forward angle of 45° relative to the beam axis and two detectors were at a backward angle of 135°. Four detectors were placed in a ring perpendicular to the beam axis. With this setup we obtained three angular correlation groups defined by the angles between the axis of the corresponding detectors of 90°, 180°, and 54.7°, which are sufficient to obtain angular correlation parameters A_0, A_2, and A_4 uniquely. A fit of the experimentally determined relative intensities in the three angular correlation groups with different hypotheses for the spin quantum numbers of the excited states and the multipolarities of the decay transitions allows the assignment of these observables. As an example, Fig. 2 shows the determination of the $E2/M1$ mixing ratio of the $2_3^+ \rightarrow 2_1^+$ transition by comparing the measured intensity ratios in the angular correlation groups to the theoretical angular correlation ratios plotted as a function of the arcus tangent of the $E2/M1$ mixing ratio δ.

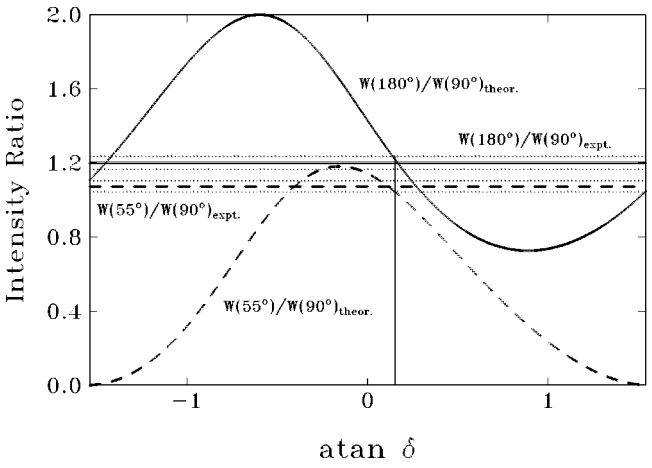

FIG. 2. Determination of multipole mixing ratios from angular correlations in the β-decay experiment. Shown are the theoretical intensity ratios of the 180° and 90° angular correlation groups $W(180°)/W(90°)$ (solid curve) and the intensity ratios of the 54.7° and 90° groups $W(55°)/W(90°)$ (dashed curve) as a function of the arctangent of the multipole mixing ratio δ for a $2^+ \rightarrow 2^+ \rightarrow 0^+$ cascade. The straight lines give the experimental results for these ratios from the $2_3^+ \rightarrow 2_1^+ \rightarrow 0_1^+$ cascade. It is clear from the diagram that for only one $M1/E2$ mixing ratio of $\delta = 0.15(4)$ both intercept points for the two different angular correlation ratios agree within the errorbars allowing a unique determination of the mixing ratio.

C. ^{91}Zr(α,n)^{94}Mo experiment

Experiments using the ''complete'' cold fusion-evaporation reaction ^{91}Zr(α,n)^{94}Mo at the Coulomb barrier were also performed at the Cologne OSIRIS cube coincidence spectrometer. We performed these measurements in order to populate medium-spin states about one to two MeV above the yrast line in ^{94}Mo. We used two different beam energies of $E_\alpha = 15$ MeV and 12 MeV. The ^{4}He beam was supplied by the Cologne FN TANDEM accelerator. In the first experiment with 15 MeV α-particle beam energy and a beam current of about 3 pnA we used an 11-mg/cm^2 zirconium target, which was enriched in ^{91}Zr to 64% with a 60-mg/cm^2 Bi backing. The beam energy was optimized to the reaction cross section. Calculations using the program code CASCADE [46] show a nearly maximum cross section for the (α,n) reaction channel at this beam energy of more than 500 mb, whereas the (α,$2n$) channel opens at about 15 MeV. The OSIRIS spectrometer was equipped with ten HPGe detectors in this experiment, six with Compton suppression shields. The ^{91}Zr(α,n)^{94}Mo reaction at $E_\alpha = 15$ MeV leads to a maximum excitation energy of $E_x^{\max} = 9.2$ MeV for the reaction product ^{94}Mo and a grazing angular momentum of $L_{\text{graz}} = 10\hbar$.

The second experiment with a 12 MeV α beam was performed with a beam current of 40 pnA due to the lower reaction cross section of about 140 mb [46]. For this experiment a zirconium target with a higher enrichment in ^{91}Zr, 89%, and a thickness of 130 mg/cm^2 was available. The beam energy was optimized for the population of low-spin states because the aim of these experiments was the investigation of low-spin MS states. In this experiment the spectrometer was equipped with five detectors with BGO Compton suppression shields and one EUROBALL CLUSTER detector [47], which has high efficiency due to its high crystal volume and use of the addback mode. Gamma-singles spectra were incremented on hard disc, and $\gamma\gamma$-coincidence events were recorded on magnetic tape with an average coincidence event rate of about 4000 events per second in the first experiment and 6000 events per second in the second.

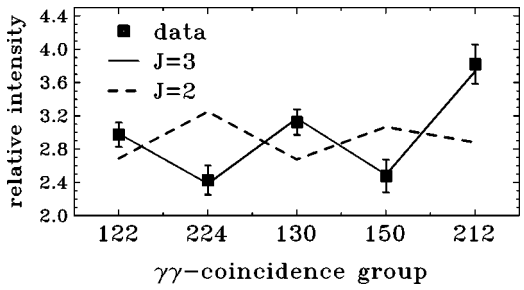

FIG. 3. Data used for the determination of the spin quantum number $J=3$ for the level at 2805.0 keV in the ^{91}Zr(α,n)^{94}Mo experiment. The solid squares show the measured relative intensities of the 1231–703-keV $\gamma\gamma$ coincidence from the $J^\pi_{2805\text{ keV}} \rightarrow 4_1^+ \rightarrow 2_1^+$ $\gamma\gamma$ cascade for five geometrically independent coincidence groups. The coincidence groups are labeled by three integers, which denote in units of $\pi/4$ the angles between the observation direction and the beam and between the planes defined by the beam and by the γ-ray direction. The lines represent the least-squares fits for the spin hypotheses $J=3$ and 2. The Gaussian width σ of the m-substate distribution and the $J^\pi_{2805\text{ keV}} \rightarrow 4_1^+$ multipole mixing ratio δ were treated as free parameters.

Spin quantum numbers of excited states and multipole mixing ratios of transitions were determined from $\gamma\gamma$ angular correlation measurements, but the situation is different from that in the β-decay experiment. In in-beam measurements the beam defines a quantization axis. For that reason we obtained five angular correlation groups defined by three angles: the angles $\theta_{1,2}$ of the two detector axis relative to the beam axis, and the angle ϕ between the planes spread out by the beam axis and emission directions of the γ rays. Figure 3 shows the relative intensities of the decay transition of a state at an excitation energy of 2805.0-keV to the 4_1^+ state in coincidence to the $4_1^+ \rightarrow 2_1^+$ transition. The experimental determined intensities were fitted with angular correlation functions using different spin hypotheses $J=2,3$. The $J^\pi_{2805.0\text{ keV}} \rightarrow 4_1^+$ multipole-mixing ratio δ and the Gaussian width σ of the m-substate distribution were treated as free parameters. The hypothesis $J=2$ for the 2805.0-keV level cannot account for the observation for any $M3/E2$ mixing ratio of the $4_1^+ \rightarrow 2_1^+$ transition whereas the hypothesis $J=3$ with a pure $4_1^+ \rightarrow 2_1^+ E2$ transition describes the data well. We obtained the best agreement for a large $E2/M1$ mixing ratio of $\delta(3^+_{2805.0\text{ keV}} \rightarrow 4_1^+) = 7.6^{+4.7}_{-3.0}$, i.e., this transition has mainly $E2$ character.

Lifetimes were extracted in the ^{91}Zr(α,n)^{94}Mo experiment using the DSAM [43]: The effective lifetimes of several short-lived states were extracted from the line shapes of their decay transitions, observed at a forward angle of 45° and a backward angle of 135° relative to the beam axis.

Because of the large number of γ-ray lines in the singles spectra, it was not possible to determine lifetimes from these spectra. Thus we analyzed the Doppler-shifted γ rays in coincidence with depopulating transitions.

The energies of γ rays emitted during the stopping process of the recoil nucleus are dependent on the angle θ of the detector relative to the actual direction of motion of the nucleus and the velocity $v(t)$ at the emission time t:

$$E_\gamma(t) = E_\gamma^0\left(1 + \frac{v(t)}{c}\cos\theta\right). \quad (7)$$

E_γ^0 is the unshifted γ-ray energy and c the speed of light. The velocity $v(t)$ is time dependent due to the stopping process in the target and includes averaging over recoil angles. A program based on the code DESASTOP [48] (also see [43]) was used to simulate the stopping process of the recoiling ^{94}Mo nuclei in the target.

The mean recoil velocity of the ^{94}Mo nuclei for $E_\alpha = 15$ MeV was $v = 0.38\%\ c$. The average stopping time in the Bi-backed ^{91}Zr target is about 700 fs in this case. We used the parameters [43] $f_n = 0.7$ for the nuclear stopping and $f_e = 1.03(0.81)$ and $a = 0.579(0.611)$ for the electronic stopping in ^{91}Zr(^{209}Bi), where f_e and a were fitted to the semiempirical stopping powers from Ref. [49] with slight modifications as described in detail in [43].

As an example, the analysis of the nearly completely Doppler-shifted transition of the 3^+ state at 2965.3 keV to the 2_2^+ state yielded an effective lifetime of $\tau_{\rm eff} = 200(30)$ fs. The effective lifetime represents an upper limit for the lifetime of the 3^+ state at 2965.3 keV because of an unknown sidefeeding. The measured Doppler shifts of the $2_3^+ \rightarrow 2_1^+$ transition show that the assumption of a prompt sidefeeding cannot be correct. From the low-energy photon scattering experiment and the $(n,n'\gamma)$ experiment with a neutron energy of 2.4 MeV, where sidefeeding of the 2_3^+ state can be excluded, a lifetime of the 2_3^+ state of $\tau = 50.8(43)$ fs was determined, whereas the lineshape analysis of the spectra from the (α,n) measurement yielded an effective lifetime of $\tau_{\rm eff} = 170(30)$ fs. Thus the only way to determine absolute lifetimes from this experiment is to employ the assumption of an equal sidefeeding time for all low-spin states in the energy range around 2–3 MeV. Using this assumption with a sidefeeding time of $\tau_{SF} = 80(20)$ fs determined from the data for the 2_3^+ state, for the 3^+ state at 2965 keV we obtain a short lifetime of $\tau = 80(30)$ fs [2]. The uncertainty is the statistical error. Not considered here is the uncertainty in the stopping power which we assume to be about 10%. The uncertainty in the determination of absolute lifetimes was the most significant motivation for the additional experiments performed on ^{94}Mo using inelastic neutron scattering, which are described in Sec. II D.

D. ^{94}Mo$(n,n'\gamma)$ experiments

Experiments on ^{94}Mo with the $(n,n'\gamma)$ reaction were performed in the 1970s [50], but no lifetimes were determined and only sparse information about spins of excited states above 2.5 MeV was available from these experiments. In addition, McEllistrem *et al.* performed $(n,n'\gamma)$ and (n,n') experiments to discover and assign excited 0^+ states in Mo isotopes [51]. In that work the 0_2^+ state in ^{94}Mo was investigated, but no higher-lying 0^+ states were identified.

The ^{94}Mo$(n,n'\gamma)$ measurements presented here were performed at the 7-MV electrostatic accelerator of the University of Kentucky. As a neutron source we used the ^{3}H$(p,n)^3$He reaction. The protons passed through a molybdenum foil into a gas cell 30 mm in length and 6.5 mm in diameter containing ^{3}H at a pressure of nearly 1 atm. The beam current of the proton beam was 2 μA and the energy spread of the neutrons was about 60 keV. The proton beam was pulsed at 2 MHz with a beam pulse width of 10 ns, then bunched to a 1-ns pulse width.

The cylindrical sample contained 36.617 g of metallic Mo powder, isotopically enriched in ^{94}Mo to 91.59 % and packed into a polyethylene container with a diameter of 26 mm and a height of 52 mm. It was suspended in the neutron flux at a distance of 65 mm from the end of the gas cell.

Gamma rays were detected with a Compton-suppressed HPGe detector with an efficiency of 55 % relative to a 3in. $\times$3in. NaI detector. The HPGe-detector and the BGO annulus detector were shielded against the neutron beam and background radiation with boron-loaded polyethylene, copper, and tungsten. The distance of the HPGe detector from the center of the sample was 1176 mm. To monitor the neutron flux incident on the ^{94}Mo sample, we placed a Hansen-McKibben long counter at 90° relative to the axis of the incident beam at 3.8 m from the sample.

Time-of-flight techniques were used to discriminate between the prompt γ rays from the $(n,n'\gamma)$ reaction in the sample and background γ rays. Further details about the neutron scattering facility, the time-of-flight measurements, neutron monitoring for normalization, and data reduction techniques have been described in Ref. [52].

In total, we performed four $(n,n'\gamma)$ measurements on ^{94}Mo. Angular distribution experiments with neutron energies of 2.4, 3.3, and 3.6 MeV were performed in which the γ rays emitted from the target were detected at 13 different angles from 40° to 155° relative to the beam axis. These experiments served to permit the measurement of lifetimes of low-lying excited states from analyzing Doppler shifts using the DSAM. The γ-ray peaks have centroids with the angular dependence

$$E_\gamma(\theta) = E_\gamma^0\left(1 + F(\tau)\frac{v_{\rm cm}}{c}\right)\cos\theta \quad (8)$$

with E_γ^0 the unshifted γ-ray energy, θ the emission angle relative to the incident beam, $E_\gamma(\theta)$ the centroid energy of a γ-ray peak at the angle θ, and $F(\tau)$ the Doppler shift attenuation factor. The theoretical $F(\tau)$ values were calculated using the theory of Winterbon [53], with slight modifications as described in [54]. The recoil velocity was $v_{\rm cm} = 8.863 \times 10^{-4} c$ in the experiment with a neutron energy of $E_{\rm n} = 3.3$ MeV and $v_{\rm cm} = 9.257 \times 10^{-4} c$ in the experiment with $E_{\rm n} = 3.6$ MeV. The measurements were performed at the above mentioned neutron beam energies to exclude sidefeeding of the states of interest from higher lying states.

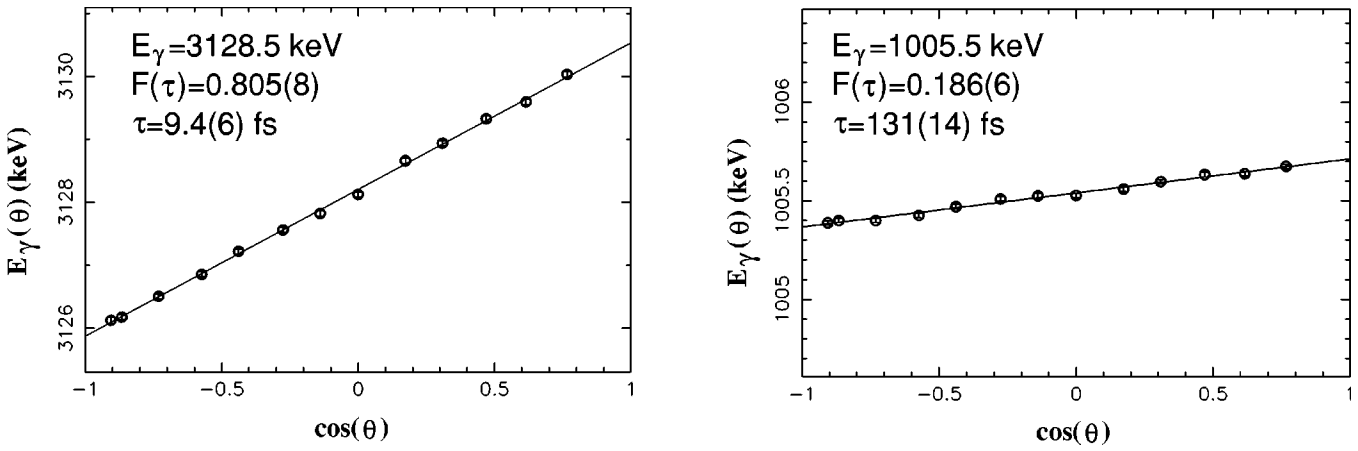

FIG. 4. Determination of lifetimes from Doppler shifts in the $(n,n'\gamma)$ angular distribution measurement. The diagram shows the Doppler shifts of the 3128.5-keV ground state transition and the decay of the 2870.0 keV level to the 2_2^+ state as a function of the cosine of the γ-ray emission angle θ relative to the direction of the incident neutrons. The experimental value of the Doppler shift attenuation factor $F(\tau)$ is determined from the slope of the best-fit line. Note the Doppler shift of the 3128.5-keV transition of about 4 keV.

As an energy standard we measured the unshifted γ rays of a ^{137}Cs source [661.660(3) kev and a ^{24}Na source [1368.675(6) and 2754.028 keV [55]] simultaneously.

As an example of the lifetime determinations from Doppler shifts, Fig. 4 shows the Doppler shift data for the ground state decay of the 3128.6-keV level and for the decay transition from the 2870.0-keV level to the 2_2^+ state in ^{94}Mo. The clearly observable Doppler shifts of many decay transitions of short-lived states allowed determinations of lifetimes in the range from a few femtoseconds up to about one ps. The errors of the lifetimes given in Table I result from both the statistical errors and the uncertainty in the stopping power. We assume this uncertainty to be about 10%.

Multipolarities of decay transitions and spins of excited states were also determined from the angular distributions of the γ rays emitted from the ^{94}Mo sample. The angular distributions were fit to even-order Legendre polynomial expansions and compared to theoretical calculations with the code CINDY [56].

Figure 5 shows data from which the spin assignment for the 2965.3-keV level and the multipole mixing ratio of the decay transition to the 2_2^+ state were determined. The left portion of Fig. 5 depicts the normalized experimental γ-ray intensities of the decay transition to the 2_2^+ state versus the emission angle relative to the incident beam axis and the fit to even-order Legendre polynomials with the parameters A_0, A_2, and A_4. The right side shows χ^2 for this fit versus the $E2/M1$ mixing ratio δ. A fit with the spin hypothesis $J=3$ for the 2965-keV level and a small $E2/M1$ mixing ratio gives the best fit.

An excitation function measurement was performed for incident neutron energies from 2.4 to 3.9 MeV. The neutron energy was increased in 100-keV steps, and each energy was measured for 12 hours. The purpose of this experiment was to place γ rays from the decay of excited states in ^{94}Mo in the level scheme and to assist in spin assignments of newly identified states. The program code CINDY [56] was used to calculate theoretical neutron scattering cross sections of excited states in ^{94}Mo, which are dependent on the energy of the incident neutrons and the spin quantum numbers. Thus a comparison with the experimentally determined neutron scattering cross sections gives information about the spins of

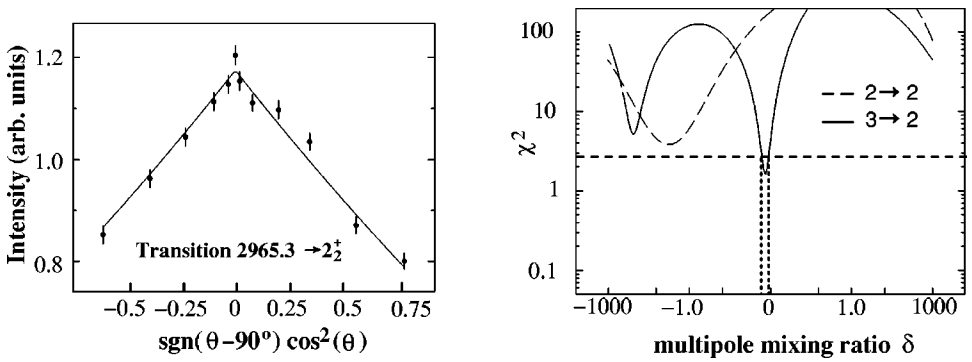

FIG. 5. Determination of the spin of the 2965.3-keV level and the multipolarity of the decay transition to the 2_2^+ state from the $(n,n'\gamma)$ angular distribution measurement. The left panel shows the angular distribution of the 1101.1-keV transition to the 2_2^+ state, including the best fit to an even-order Legendre polynomial with the parameters A_0, A_2, and A_4. The right panel depicts χ^2 for this fit vs the $E2/M1$ mixing ratio δ for initial spin states of $J=2,3$. The experimental uncertainty is obtained from accepting δ values that yield $\chi^2 \leq \chi^2_{\min}+1$.

TABLE I. Levels and transitions in ^{94}Mo. The table contains the level and transition energies, the spins of the corresponding states, relative intensities I_γ, multipole mixing ratios δ, and lifetimes τ of the excited states. Those lifetimes, which are marked with "eff," were only determined in the (α,n) experiment and are effective lifetimes because of an unknown sidefeeding. Uncertainties are given in the last digits. The last column gives the experiments in which the excited states were observed. "A" refers to the photon scattering experiment, "B" to the β-decay measurement, "C" to the ^{91}Zr$(\alpha,n)^{94}$Mo reaction, and "D" to the ^{94}Mo$(n,n'\gamma)$ experiment. The excitation energies of newly identified states and transition energies of newly observed transitions are marked with "n." If two values for the multipole mixing ratio δ are given, the determination was ambiguous.

E_x (keV)	J_i^π	J_f^π	E_γ (keV)	I_γ (%)	$\delta(J_i^\pi \to J_f^\pi)$	τ (fs)	Expt.
871.09(10)	2_1^+	0_1^+	871.09(10)	100.0	0	4150(60)[a]	B C D
1573.72(14)	4_1^+	2_1^+	702.63(10)	100.0	0.00(4)	7210(1000)[a]	B C D
1864.3(1)	2_2^+	0_1^+	1864.3(2)	10.3(10)	0	402^{+86}_{-75}	B C D
		2_1^+	993.1(1)	100.0(10)	$-2.0(10)$		
2067.4(1)	2_3^+	0_1^+	2067.4(1)	15.1(7)	0	50.8(43)	A B C D
		2_1^+	1196.2(1)	100.0(7)	0.15(4)		
2294.7(2)	4_2^+	2_1^+	1423.7(3)	13.3(2)	0.08(8)	109(16)	B C D
		4_1^+	721.0(2)	100.0(2)	0.03(4)		
2393.1(1)	2_4^+	0_1^+	2393.1(1)	11.11(22)	0	120^{+17}_{-15}	A B C D
		2_1^+	1521.8(1)	100.0(20)	$-0.12(3)$		
		2_2^+	528.7(3)	0.719(33)	-		
		2_3^+	325.7(3)	0.61(14)	-		
2423.4(2)	6_1^+	4_1^+	849.7(1)	100.0	$-0.04(5)$	>450	B C D
2533.8(3)	3_1^-	2_1^+	1662.7(3)	100.0(22)	0.03(7)	750^{+130}_{-110}	B C D
		4_1^+	960.1(3)	81.3(31)	0.00(2)		
		2_2^+	669.6(2)	31.9(13)	$-0.03(13)$		
		2_3^+	466.4(3)	57.3(10)	0.00(3)		
2564.9(3)	4_3^+	2_1^+	n 1693.9(7)	11.8(8)	$-0.01(10)$	226^{+70}_{-49}	C D
		4_1^+	991.2(2)	100.0(8)	$0.10^{+0.25}_{-0.17}$		
2610.5(2)	5_1^-	4_1^+	1036.8(2)	100.0	0.00(4)	640^{+160}_{-110}	B C D
2739.9(1)	1_1^+	0_1^+	2739.9(1)	65.4(13)	0	77(7)	A B D
		2_1^+	1868.8(1)	100.0(20)	$-0.12(2)$		
		0_2^+	998.2(2)	4.44(10)	0		
		2_2^+	875.5(2)	24.4(5)	$-0.10(2)$		
		2_3^+	672.0(7)	3.02(48)	-		
2768.2(2)	4_4^+	2_1^+	1896.5(2)	100.0(38)	0.02(3)	155(17)	C D
		4_1^+	n 1193.8(5)	71.2(38)	-		
n 2780.5(2)	0_3^+	2_2^+	n 916.2(2)	100.0	0	480^{+120}_{-90}	D
2805.0(3)	3_1^+	2_1^+	1933.9(4)	75.7(30)	$-0.66(14)$	508^{+76}_{-63}	C D
					$-1.7^{+0.4}_{-0.5}$		
		4_1^+	1231.2(3)	100.0(53)	$7.6^{+4.7}_{-3.0}$		
		2_2^+	940.7(4)	62.9(39)	$2.3^{+0.7}_{-0.5}$		
2834.8(5)	(4_1^-)	4_1^+	1261.1(5)	100.0	0.06(7)	>1000	C D
		3_1^-	n 301.1(3)	13.1(12)	0.12(10)		
		5_1^-	n 224.2(5)	7.2(10)	$3.3^{+1.0}_{-1.9}$		
					0.18(12)		
2870.0(2)	2_5^+	0_1^+	2870.0(2)	17.3(5)	0	131(14)	B C D
		2_1^+	1998.9(2)	13.1(6)	$1.3^{+1.4}_{-0.4}$		
		2_2^+	1005.5(1)	100.0(36)	$-0.05(4)$		
		2_3^+	802.6(2)	26.2(15)	-		
2872.4(2)	6_2^+	6_1^+	449.0(1)	100.0	0.14(6)	$>1000^{\text{eff}}$	B C D
2955.5(3)	(8_1^+)	6_1^+	532.1(1)	100.0	$-0.03(5)$	141(3) ns[a]	B C
2965.3(2)	3_2^+	2_1^+	2094.3(1)	36.9(14)	$1.1^{+1.0}_{-0.4}$	79(8)	B C D
		4_1^+	1391.6(1)	63.0(24)	$-0.08(6)$		

TABLE I. (*Continued*).

E_x (keV)	J_i^π	J_f^π	E_γ (keV)	I_γ (%)	$\delta(J_i^\pi \rightarrow J_f^\pi)$	τ (fs)	Expt.
		2_2^+	1101.1(1)	100.0(23)	$-0.09(6)$		
		2_3^+	898.1(1)	23.0(12)	$2.0^{+1.2}_{-0.6}$		
					0.39(25)		
2993.1(3)	2_6^+	0_1^+	n 2993.0(10)	6.76(88)	0	218^{+27}_{-25}	C D
		2_1^+	2122.0(3)	63.7(15)	$-2.6^{+0.6}_{-0.7}$		
		2_2^+	1128.6(5)	100.0(38)	$-3.4^{+0.7}_{-0.9}$		
		2_3^+	n 925.8(3)	45.0(26)	$-0.07^{+0.07}_{-0.06}$		
3011.5(2)	3_2^-	2_1^+	2140.4(2)	100.0(23)	0.03(5)	320^{+90}_{-60}	C D
		4_1^+	1437.6(5)	36.7(27)	0.04(6)		
		2_2^+	1147.3(5)	11.5(15)	0.01(6)		
		2_3^+	n 944.3(6)	11.9(16)	-		
		3_1^-	477.5(5)	50.9(17)	$-0.10(19)$		
n 3026.8(4)	(3)	3_1^-	n 493.0(2)	60.1(36)	-	>780	D
		5_1^-	n 416.4(3)	100.0(36)	-		
n 3072.4(3)	$(2,3^+)$	2_1^+	n 2201.3(3)	37.3(22)	-	510^{+100}_{-80}	D
		2_2^+	n 1208.1(2)	100.0(52)	-		
		3_1^-	n 538.5(7)	11.5(23)	-		
3082.4(3)	(3_3^+)	2_1^+	2211.3(3)	100.0(21)	$-0.01(6)$	980^{+400}_{-240}	C D
		2_2^+	1218.2(4)	14.2(21)	0.09(5)		
3128.6(2)	1_2^+	0_1^+	3128.5(2)	100.0(3)	0	9.4(6)	A B D
		2_1^+	2257.6(1)	4.29(10)	$0.74^{+0.21}_{-0.17}$		
		2_2^+	1264.3(1)	18.27(37)	$-0.08(3)$		
		2_3^+	1061.1(5)	1.16(11)	$-7.0^{+3.0}_{-20.0}$		
					$-0.57(16)$		
3163.3(3)	(3_4^+)	2_1^+	2292.2(2)	100.0(13)	0.17(4)	91(10)	B C D
		3_1^+	n358.0(5)	16.7(13)	$-0.35(12)$		
3165.8(2)	6_3^+	4_1^+	1592.0(1)	100.0(35)	$-0.01(6)$	465(50) [eff]	B C
		6_1^+	742.2(2)	29.4(11)	0.15(7)		
		6_2^+	293.4(1)	79.4(25)	0.18(5)		
3201.0(3)	(4)	4_2^+	906.3(2)	100.0(22)	0.00(6)	63^{+8}_{-7}	C D
		4_1^+	n 1627.4(5)	29.4(22)	0.2(2)		
n 3243.1(5)	(5_1^+)	4_1^+	n 1669.4(5)	100.0	0.71(14)	133^{+23}_{-21}	C D
3260.8(5)	1_1^-	0_1^+	3260.7(5)	100.0	0	57(6)	A D
3307.1(4)	2_7^+	2_1^+	2436.0(4)	100.0	$-4.0^{+1.1}_{-2.4}$	580^{+200}_{-130}	C D
					0.03(8)		
3320.7(5)	(9)	(8_1^+)	365.2(3)	100.0	2.2(3)	>1000 [eff]	C
n 3331.7(3)	(3^+)	2_1^+	n 2460.8(8)	7.4(11)	-	75(9)	B C D
		4_1^+	n 1758.0(2)	100.0(55)	$-0.10(3)$		
		2_2^+	n 1467.3(3)	47.9(29)	$0.3^{+2.9}_{-0.2}$		
3339.6(3)	6_4^+	6_1^+	916.2(1)	100.0	0.02(7)	182(30) [eff]	B C
n 3366.4(7)	$(3^+,4)$	4_2^+	n 1071.6(5)	100.0(35)	-	880(100) [eff]	C
		3_2^+	n 401.1(5)	23.7(35)	-		
3366.9(10)	$(5,7^-)$	5_1^-	756.5(7)	100.0	-	>1000 [eff]	C
n 3371.1(5)	(2,3,4)	4_1^+	n 1797.4(5)	100.0(73)	-	200^{+100}_{-60}	D
		2_3^+	n 1303.7(7)	26.1(42)	-		
		4_3^+	n 806.1(5)	93.2(76)	-		
		3_2^+	n 405.8(5)	82.6(66)	-		
3389.5(7)	$5_2^{(-)}$	4_2^+	n 1094.6(5)	100.0	$-0.01(3)$	700(180) [eff]	C
n 3398.2(4)	(3,4)	4_1^+	n 1824.5(4)	100.0	-	51^{+10}_{-9}	C D
n 3400.8(2)	-	2_1^+	n 2529.7(3)	100.0(8)	-	33(4)	D

TABLE I. (*Continued*).

E_x (keV)	J_i^π	J_f^π	E_γ (keV)	I_γ (%)	$\delta(J_i^\pi \rightarrow J_f^\pi)$	τ (fs)	Expt.
		2_2^+	n 1536.5(2)	4.2(8)	-		
3429.1(9)	-	2_1^+	2558.0(8)	100.0	-	-	D
3447.6(5)	(2)	0_1^+	3447.5(10)	5.1(3)	0	51^{+7}_{-6}	B C D
		2_1^+	2576.5(5)	100.0(3)	$-1.9^{+0.5}_{-0.6}$		
					$-0.08(10)$		
n 3448.2(5)	(5_2^+)	4_1^+	n 1874.6(5)	100.0(66)	$-0.75(25)$	650(200) [eff]	C
		6_2^+	n 576.7(5)	33.1(66)	0.03(5)		
3511.7(2)	$1_3^{(+)}$	0_1^+	3511.6(2)	100.0(11)	0	13^{+8}_{-4}	A B D
		2_1^+	2640.7(3)	51.6(13)	-		
		0_2^+	1770.4(2)	48.6(92)	0		
n 3532.3(7)	(1,2)	0_1^+	n 3532.0(10)	19.8(25)	-	-	D
		2_1^+	n 2660.1(10)	100.0(79)	-		
		0_2^+	n 1789.8(5)	78.2(54)	-		
3534.3(2)	2_8^+	0_1^+	3534.0(4)	5.09(55)	0	150(40) [eff]	B C
		2_1^+	2663.2(2)	100.0(23)	$-0.3(2)$		
		2_2^+	1670.0(1)	56.1(20)	0.15(19)		
n 3588.3(7)	-	5_1^-	n 978.0(5)	100.0	-	-	D
n 3693.1(11)	(3,4)	2_1^+	n 2822.1(15)	95(22)	-	150(50) [eff]	C
		4_4^+	n 925.8(5)	100(22)	-		
3792.8(3)	2_9^+	0_1^+	3792.3(10)	77.8(20)	0	-	B
		2_2^+	1928.5(2)	100.0(40)	-		
		2_4^+	1399.9(2)	54.9(30)	-		
3805.1(6)	(8,10)	(9)	484.4(5)	100.0	-	>1000 [eff]	C
3847.3(10)	(2,3,4)	4_2^+	1552.5(7)	100.0	-	190(40) [eff]	C
3866.8(4)	(9)	(8_1^+)	911.3(4)	100.0	$6.6^{+3.3}_{-1.6}$	>1000 [eff]	C
3892.2(2)	(2^+)	0_1^+	3891.6(10)	17.4(9)	-	-	B
		2_1^+	3021.0(1)	100.0(24)	-		
		2_2^+	n 2027.9(2)	22.3(10)	-		
		2_3^+	n 1824.9(3)	25.8(10)	-		
		2_4^+	n 1499.1(1)	79.4(22)	-		
n 3897.9(10)	$(3^+,5^+)$	4_2^+	n 1602.7(10)	100.0	-	113(40) [eff]	C
n 3932.4(7)	(7_1^+)	6_1^+	n 1508.9(7)	100.0	2.45(28)	182(30) [eff]	C
					0.38(4)		
n 4105.5(11)	-	4_2^+	n 1810.7(10)	100.0	-	130(40) [eff]	C
n 4237.5(15)	-	4_2^+	n 1942.7(12)	100.0	-	90(40) [eff]	C

[a]Lifetimes taken from Ref. [57].

excited states. Figure 6 displays the data and calculation for the 2739.9 and 2780.5-keV levels.

III. LEVEL DISCUSSION

Experimental information for all the observed levels is provided in Table I; those states which are of special interest are discussed in detail below.

2_3^+ state at 2067.4 keV. Spin and parity of this state were known previously [57]. The spin assignment was confirmed in all experiments, and the positive parity is clear because of a fast quadrupole transition to the ground-state. From the photon scattering experiment and the neutron scattering experiment with $E_n = 2.6$ MeV, we obtain a mean value for the lifetime of $\tau(2_3^+) = 50.8(43)$ fs. The β^+ decay experiment, the (α,n) experiment, and the neutron scattering measurement yielded a consistent value for the multipole mixing ratio of the $2_3^+ \rightarrow 2_1^+$ transition, resulting in predominantly $M1$ character. This result shows that a previous ^{94}Mo$(p,p'\gamma)$ measurement [57,58] was in error.

4_2^+ state at 2294.7 keV. This state was known from previous experiments [57]. In addition to the known decay transition to the 4_1^+ state, a fast transition to the 2_1^+ state was observed and supports the spin and parity assignment from [57]. The spin assignment $J=4$ was confirmed in our angular correlation measurements and positive parity is assigned because a fast $M2$ decay to the 2_1^+ state can be excluded. This state decays predominantly by a strong $M1$ transition to the 4_1^+ state.

4_3^+ state at 2564.9 keV. The 4_3^+ state was previously

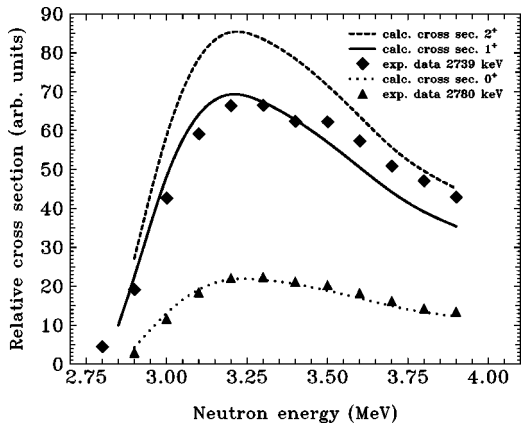

FIG. 6. Excitation function of two excited states in ^{94}Mo populated by the $(n,n'\gamma)$ reaction. Shown are comparisons of the experimentally determined neutron scattering cross sections to the results of a calculation using the code CINDY [56]. For the 2739.9-keV level, the neutron scattering cross sections are calculated both for the spin hypotheses $J=1,2$ for the 2780.5 keV level for the spin hypothesis $J=0$. The excited state at 2739.9 keV was clearly identified as a $J=1$ state, while the 2780.5-keV level represents a $J=0$ state. The angular distribution analysis supports these spin assignments.

placed at 2566.8 keV [57], however, the only recently identified decay transition is that to the 4_1^+ state with a transition energy of 993.1(8) keV. Thus this peak should form a doublet with the strong $2_2^+ \rightarrow 2_1^+$ transition of the same energy. In the γ-ray spectra of the ^{91}Zr$(\alpha,n)^{94}$Mo and $(n,n'\gamma)$ reactions, a peak at 991.2(2) keV at the side of the 993.1 keV $2_2^+ \rightarrow 2_1^+$ line was observed. From the $\gamma\gamma$ coincidence data we can interprete this peak as arising from the decay of an excited state at 2564.9(3) keV to the 4_1^+ state. From the $(n,n'\gamma)$ data, we established a small $E2/M1$ mixing ratio for the transition to the 4_1^+ state for the spin assignment $J=4$. In addition, we observed a decay transition to the 2_1^+ state with about 12 % the intensity of the transition to the 4_1^+ state. The best fit for a small mixing ratio consistent with zero for the spin hypothesis $J=4$ confirms the spin and parity assignment 4^+. Thus we identify the excited state at 2564.9(3) keV with the 4_3^+ state.

1_1^+ state at 2739.9 keV. This state was known before as a $J^\pi=(1,2)^+$ state [57]. In our recent publication [1] spin and parity $J^\pi=2^+$ was assigned to this state from the analysis of the angular distribution data in the photon scattering experiment, whereas the γ-ray line from the ground state decay, from which the spin was determined, was a doublet with the 2734.9-keV γ ray of the calibration standard ^{27}Al in that measurement and very weak in intensity. Thus this state was interpreted as the 2_5^+ state in [1]. The data from the ^{94}Mo$(n,n'\gamma)$ experiment yielded clearly spin $J=1$. Positive parity is strongly favored due to the strong population of this state in the β decay experiment with a log ft value of log $ft=5.1$ for the β decay from the (2^+) isomer of ^{94}Tc. Therefore, we reassign the state at 2739.9 keV as the 1_1^+ state.

4_4^+ state at 2768.2 keV. This state was observed in agreement with the data from Ref. [57]. The spin assignment was confirmed from our data. For the first time, a decay transition to the 4_1^+ state was observed. Since this transitions forms a doublet with the strong $2_3^+ \rightarrow 2_1^+$ transition at 1196.2 keV, we were not able to evaluate the $E2/M1$ mixing ratio.

0_3^+ state at 2780.5 keV. A new state was identified at an excitation energy of 2780.5(2) keV from its lone decay transition to the 2_2^+ state. The $\gamma\gamma$ angular correlation measurements allow the spin assignments $J=0,1,2$, but from the $(n,n'\gamma)$ excitation function measurement we assigned clearly spin $J=0$ (see Fig. 6). Because of the rather strong decay transition to the 2_2^+ state we assume positive parity, thus this newly observed state is the 0_3^+ state in ^{94}Mo.

3_1^+ state at 2805.0 keV. A state with spin and parity $J=2^+,3^+$ had been identified at this energy [57]. The positive parity assignment stems from an ^{95}Mo$(d,t)^{94}$Mo experiment, where an $l=0$ angular momentum transfer was measured for this level [59], thus $J^\pi=3^+$ was suggested. From the angular correlations of the decay transitions to the 2_1^+, 4_1^+, and 2_2^+ states, we assigned spin $J=3$ unambiguously.

2_5^+ state at 2870.0 keV. In an (p,p') experiment [60] an excited state with spin and parity $J^\pi=2^+$ was placed at 2868(5) keV. In a previous ^{94}Mo$(n,n'\gamma)$ experiment [50], a $J^\pi=(2^+)$ state at an energy of 2870.7(9) keV was observed. The observation of an excited state at 2870.0(2) keV with spin $J=2$ in the β-decay experiment, in the ^{91}Zr$(\alpha,n)^{94}$Mo reaction, and in the $(n,n'\gamma)$ study provides evidence that this state is the same state which was observed in the (p,p') measurement at 2868 keV and in the previous $(n,n'\gamma)$ experiment at 2870.7 keV. Positive parity can be confirmed because a fast ground state transition was observed.

3_2^+ state at 2965.3 keV. The spin and parity assignment was done in [2]. The $3^+ \rightarrow 4_1^+, 2_2^+$ transitions have almost pure $M1$ character, whereas the $3^+ \rightarrow 2_1^+, 2_3^+$ transitions may have considerable $E2$ admixtures (see detailed discussion in Sec. IV). A lifetime of $\tau=79(8)$ fs was determined in the $(n,n'\gamma)$ experiment in agreement with the value from the ^{91}Zr$(\alpha,n)^{94}$Mo experiment corrected for unobserved sidefeeding of $\tau_{(\alpha,n)}(3_2^+)=80(30)$ fs [2].

3_2^- state at 3011.5 keV. The data from the $(\alpha,$n$)$ and ^{94}Mo$(n,n'\gamma)$ experiments confirm the spin assignment $J=3$ from [57]. Our data allow negative parity due to small multipole mixing ratios of the transitions to the 2_1^+, 2_2^+, and 4_1^+ states which are consistent with zero, thus allowing pure $E1$ transitions. The negative parity was determined from a ^{92}Mo$(p,t)^{94}$Mo experiment, where an angular momentum transfer of $L=3$ was measured for a state at 3014(12) keV [61], which can be identified with the excited state at 3011.5 keV.

1_2^+ state at 3128.6 keV. In the photon scattering experiment a strong dipole excitation at 3128.3(5) keV was observed. Positive parity was already known for this state from previous (p,p') and (d,d') experiments [62], but spin $J=2$ was assigned in those measurements. The angular distributions of the γ rays in the photon scattering and the $(n,n'\gamma)$ experiments give clear evidence for a dipole excited

state. The β-decay experiment yielded the branching ratios shown in Table I for the four observed decay transitions of the 1_2^+ state and the corresponding multipole mixing ratios. The decay to the 2_2^+ state represents a nearly pure $M1$ transition. The decay to the 2_1^+ state has a higher $E2$ admixture associated with a larger $E2/M1$ mixing ratio. No clear value for the $E2/M1$ mixing ratio of the $1_2^+ \rightarrow 2_3^+$ transition was established, the data yielded two different values pointing to some $E2$ admixture. In the ^{91}Zr$(\alpha,n)^{94}$Mo reaction no decay transitions of the 1_2^+ state were clearly identified.

1_1^- state at 3260.8 keV. An excited state with spin and parity $J^\pi = 1^-$ was found previously at 3263.8(17) keV [57]. In the photon scattering experiment with an endpoint energy of the bremsstrahlung spectrum of 4.0 MeV, we observed a state with spin $J=1$ at 3260.8(5) keV. The fact that this state was not observed in the β-decay experiment gives an indication of negative parity, because negative parity states were populated very weakly compared to positive parity states. Also in the $(n,n'\gamma)$ experiment a ground state transition of a $J=1$ state at the same energy was observed. Since no hint for another dipole excitation was found in this energy region we identify the 3260.8 keV state with the 1_1^- state.

$1_3^{(+)}$ state at 3511.7 keV. A state with spin $J=1$ was observed in photon scattering, in the β-decay experiment, and in the excitation function measurement with the $(n,n'\gamma)$ reaction. The state was not populated in the $(n,n'\gamma)$ angular distribution measurements, because it lies too close to the highest used neutron energy of 3.6 MeV. No information about the multipolarity of the transition to the 2_1^+ state was determined. We identify this state with the $J^\pi = (1,2^+)$ state at 3512.7(11) keV from [57]; thus we assume a probable positive parity.

IV. MIXED-SYMMETRY STATES

In the following we discuss the identification of the one-Q-phonon $2_{1,\mathrm{ms}}^+$ state and the 1^+,2^+, and 3^+ two-Q-phonon MS states in ^{94}Mo with the structure $(2_1^+ \otimes 2_{1,\mathrm{ms}}^+)$ from the measurement of absolute transition strengths. A comparison of our data to theoretical predictions in the framework of the IBM-2 will be given. Some discussion about the identification of MS states in ^{94}Mo was recently published by our group [1–3]. Later, we will briefly show an interpretation of the observed MS states in the spherical shell model [4] and in the quasiparticle phonon model (QPM) [5,6] from recent work.

A. One-Q-phonon $2_{1,\mathrm{ms}}^+$ state

Figure 7 displays measured $E2$ and $M1$ transition strengths which are relevant for the identification of the one-Q-phonon $2_{1,\mathrm{ms}}^+$ state. For the 2_1^+ state the $E2$ excitation strength has been taken from [57], all other data are from this work.

The top half of Fig. 7 depicts the $M1$ transition strengths of the lowest seven observed nonyrast 2^+ states to the 2_1^+ state. Only the 2_3^+ state decays via an enhanced $M1$ transition to the 2_1^+ state with a transition matrix element of

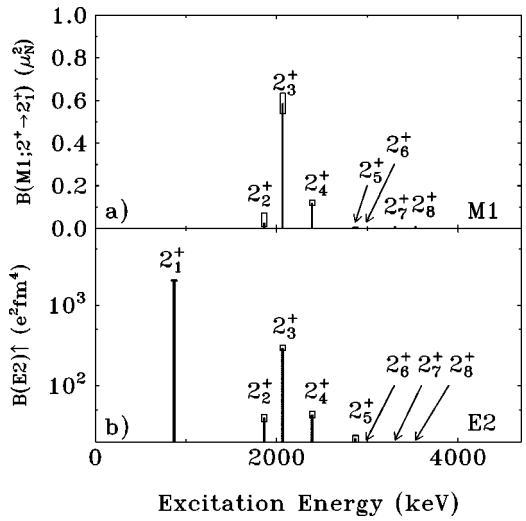

FIG. 7. Measured $E2$ and $M1$ strengths relevant for the identification of the $2_{1,\mathrm{ms}}^+$ state in ^{94}Mo. Panel (a) shows the $B(M1;2^+ \rightarrow 2_1^+)$ values for the seven lowest identified nonyrast 2^+ states, and panel (b) shows the $E2$ excitation strengths for all clearly identified 2^+ states. The error bars are displayed as boxes.

$|\langle 2_1^+ \| M1 \| 2_3^+ \rangle| = 1.7(1)\mu_N$, which agrees with the predictions of the IBM-2 for a one-Q-phonon MS state. Therefore, we interprete the 2_3^+ state as the one-Q-phonon $2_{1,\mathrm{ms}}^+$ state. Because no other 2^+ state shows a comparable strong $M1$ decay to the 2_1^+ state, the $2_{1,\mathrm{ms}}^+$ state in ^{94}Mo is nearly unfragmented.

The $E2$ excitation strength distribution, shown in the lower half of Fig. 7 (remark the logarithmic scale), is dominated by the 2_1^+ state, the *pn* symmetric one-Q-phonon excitation. The excitation strength of the 2_3^+, the $2_{1,\mathrm{ms}}^+$ state amounts to about 10% of the $0_1^+ \rightarrow 2_1^+$ strength, but, on the other hand, it is about one order of magnitude larger than the $E2$ excitation strength to the 2_2^+ state, which has the characteristics of a symmetric two-Q-phonon state. This gives evidence that the 2_3^+ state represents a one-Q-phonon state. None of the other observed 2^+ states above the 2_1^+ state shows a comparably strong $E2$ excitation strength.

B. Identification of the two-Q-phonon 1_{ms}^+ state

Three 1^+ states have been identified in ^{94}Mo. The total $M1$ strength from the ground state to the 1^+ states at 2739.9, 3128.6, and 3511.7 keV is $\Sigma B(M1)\uparrow = 0.67(7)\ \mu_N^2$, whereas the 1_2^+ state at 3128.6 keV represents the strongest fragment. Figure 8 shows the $M1$ excitation strength distribution in ^{94}Mo. The weighted average energy lies at 3.2 MeV. These data fit well into the systematics of the 1^+ scissors mode observed so far. From the empirical formulas [26,37,39] extracted from data for the 1_{ms}^+ state in the rare earth region, we expect the 1_{ms}^+ scissors mode in ^{94}Mo at an excitation energy of 3.2–3.5 MeV with a total excitation strength of $B(M1)\uparrow \approx 0.55\ \mu_N^2$. This agrees with our observations within two standard deviations.

Moreover, the 1_2^+ state shows clear signatures of a two-Q phonon MS state as predicted in the IBM-2: According to the

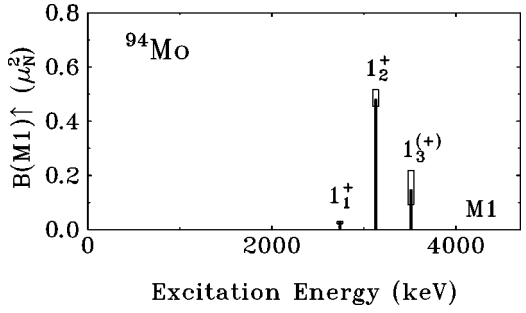

FIG. 8. Measured $M1$ excitation strengths of all observed 1^+ states relevant for the identification of the $1^+_{\rm ms}$ state in ^{94}Mo. The 1^+_2 state dominates the $M1$ strength distribution. The boxes give the error bars.

Q-phonon scheme [see Eqs. (2)–(5)] the MS Q phonon $Q_{\rm m}$ is annihilated both in the $2^+_{1,\rm ms}\rightarrow 0^+_1$ and in the $1^+_{\rm ms}\rightarrow 2^+_1$ transition, respectively. Therefore, the $1^+_{\rm ms}\rightarrow 2^+_1$ decay should be a weakly collective $E2$ transition. In fact, we get a transition strength of $B(E2;1^+_2\rightarrow 2^+_1)=0.72^{+0.27}_{-0.24}$ W.u., and only a small $M1$ admixture in agreement with the Q-phonon scheme. The $1^+_{\rm ms}\rightarrow 2^+_{1,\rm ms}$ decay results in the Q-phonon scheme from the annihilation of the symmetric Q-phonon $Q_{\rm s}$. Thus we expect this decay to be a collective $E2$ transition. The ^{94}Mo$(n,n'\gamma)$ experiments yielded two different $E2/M1$ mixing ratios. One is consistent with nearly pure $E2$ radiation. Under the assumption of pure $E2$ radiation, we determine an $E2$ transition strength comparable to the strength of the collective $2^+_1\rightarrow 0^+_1$ decay. The latter $E2/M1$ mixing ratio yields an $E2$ strength of $B(E2;1^+_2\rightarrow 2^+_3)=5.9^{+3.3}_{-2.8}$ W.u. Therefore, in any case, the $E2$ transition strength of the $1^+_2\rightarrow 2^+_3$ decay is larger than 3 W.u., giving evidence for the expected collectivity of this decay.

For γ soft nuclei, $M1$ transitions obey selection rules [63] with respect to the d-parity quantum number $\pi_d=(-1)^{n_Q}$, i.e., the number of Q-phonons n_Q modulo 2 does not change. According to Eqs. (2)–(5) the $M1$ transitions from the $1^+_{\rm ms}$ state to the 2^+_1 and $2^+_{1,\rm ms}$ state, respectively, are d parity forbidden, whereas the $1^+_{\rm ms}\rightarrow 2^+_2$ transition is allowed. The 1^+_2 state possesses the strongest $1^+\rightarrow 2^+_2$ $M1$ decay of the observed 1^+ states, characteristic for a two-Q-phonon $1^+_{\rm ms}$ state (see the upper part of Fig. 9). The measured ratio of the $M1$ strengths of the $1^+_2\rightarrow 2^+_1$ and $1^+_2\rightarrow 2^+_2$ transitions amounts to 0.03, well confirming the d-parity selection rule on a few percent level. Due to the ambiguous $E2/M1$ mixing ratio of the $1^+_2\rightarrow 2^+_3$ transition a similar confirmation for the d-parity selection rule for $M1$ transitions is not possible for this decay. To conclude, we identify the 1^+_2 state as the main fragment of the two-Q-phonon $1^+_{\rm ms}$ state in ^{94}Mo [1].

C. Two-Q-phonon $2^+_{2,\rm ms}$ state

At an excitation energy of 2870.0 keV the 2^+_5 state was observed. In our recent publication [3], this state was designated as the 2^+_6 state due to the erroneous interpretation of the 2739.9-keV level as the 2^+_5 state discussed above. But

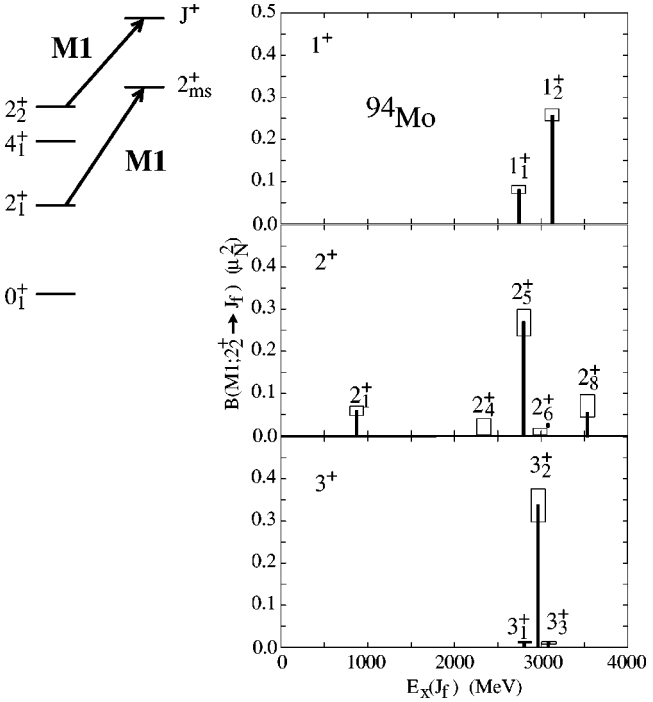

FIG. 9. $M1$ transition strengths from the 2^+_2 state to 1^+ states (upper panel), 2^+ states (middle panel), and 3^+ states (lower panel) in ^{94}Mo. The bars give the transition strengths, and the open boxes show the experimental uncertainties. No transitions from the 1^+_3, 2^+_3, 2^+_7, and (3^+_4) states to the 2^+_2 state were observed. For the 2^+_4 state at 2393 keV, only an upper limit for the $M1$ transition strength was determined. The 1^+_2, 2^+_5, and the 3^+_2 states can be clearly identified as two-Q-phonon MS states.

the data from the recently performed ^{94}Mo$(n,n'\gamma)$ experiments clearly show that the 2739.9-keV level represents a $J=1$ state.

The 2^+_5 state at 2870 keV is identified as the two-Q-phonon $2^+_{2,\rm ms}$ state, because it is the only observed 2^+ state fulfilling the signatures from the IBM-2 for this state: It decays with a strong $M1$ transition to the symmetric 2^+_2 state with a transition matrix element of $|\langle 2^+_2\|M1\|2^+_5\rangle|=1.16(6)\ \mu_N$.

In our measurements on ^{94}Mo we were able to observe a total of ten 2^+ states. For seven of these, we obtained lifetime information. The lifetime of the 2^+_1 state was previously known. The highest observed 2^+ states, the 2^+_9 state at 3792.8 keV, and the (2^+_{10}) state at 3892.2 keV, were only observed in the β-decay experiment; therefore, we have no lifetime information for these states. From the lifetimes, the measured branching ratios, and $E2/M1$ multipole mixing ratios, we deduced the $M1$ transition strengths for the $2^+_x\rightarrow 2^+_2$ transitions. We determined the 2^+_5 state as clearly having the largest $M1$ transition strength to the 2^+_2 state (see the middle part of Fig. 9). In addition, for a two-Q-phonon 2^+ MS state, we expect a weakly collective $E2$ decay to the 2^+_1 state from the annihilation of the MS Q phonon $Q_{\rm m}$. In fact, we determined a weakly collective $2^+_5\rightarrow 2^+_1$ $E2$ transition strength. Due to the large errorbars of the $E2/M1$ mixing ratio of the $2^+_5\rightarrow 2^+_3$ transition, we cannot give a definite

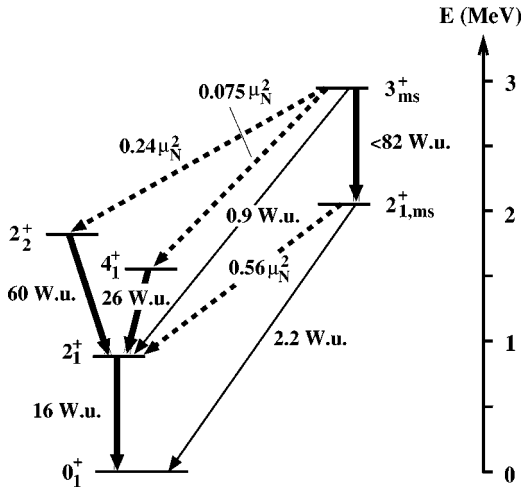

FIG. 10. Decay transitions of the 3_2^+ state including the transition strengths relevant for the clear identification of this state as a two-Q-phonon MS state. The solid arrows stand for transitions having predominantly $E2$ character; the dashed arrows represent those with $M1$ character. $E2$ strengths are given in Weisskopf units; $M1$ strengths are in μ_N^2.

value for the $E2$ strength of this decay. We determined an upper limit of $B(E2;2_5^+ \rightarrow 2_3^+) < 140$ W.u. This agrees with the collective $E2$ transition expected for the $2^+_{2,\mathrm{ms}} \rightarrow 2^+_{1,\mathrm{ms}}$ transition.

These observations lead to the conclusion, that the 2_5^+ state has the properties of a two-Q-phonon $2^+_{2,\mathrm{ms}}$ state [3]. It should be stressed that this is the first identification of a two-Q-phonon $2^+_{2,\mathrm{ms}}$ state from absolute $M1$ and $E2$ transition strengths.

D. Two-Q-phonon 3^+_{ms} state

The 3_2^+ state at 2965.3 keV can be clearly identified as the 3^+ two-Q-phonon MS state from its decay properties [2] (see Fig. 10). Strong $M1$ decays with matrix elements of the order of about 1 μ_N were observed for the decay transitions to the symmetric two-Q-phonon states. Using the lifetime, the branching ratios, and the $E2/M1$ mixing ratios, we determine that both the decay transitions to the 2_2^+ state and to the 4_1^+ state represent strong $M1$ transitions with transition matrix elements of $|\langle 2_2^+ \| M1 \| 3_2^+ \rangle| = 1.30(8)\ \mu_N$ and $|\langle 4_1^+ \| M1 \| 3_2^+ \rangle| = 0.72(5)\ \mu_N$, respectively. These large matrix elements are signatures for MS character (see Fig. 10). In addition, the bottom part of Fig. 9 depicting the $2_2^+ \rightarrow 3^+$ $M1$ transition strengths of all observed $3^+ \rightarrow 2_2^+$ transitions shows that the 3_2^+ state is the only level exhibiting this clear characteristics of a 3^+_{ms} state.

The $3_2^+ \rightarrow 2_1^+$ $E2$ transition is weakly collective with a transition strength of about one Weisskopf unit. Such a value is actually expected for a transition from a two-Q-phonon MS state to the 2_1^+ state due to the annihilation of Q_{m}. The $3_2^+ \rightarrow 2_3^+$ transition is consistent with a collective $E2$ strength with tens of Weisskopf units as expected for a transition resulting from the annihilation of Q_{s}. The uncertainty of the multipole mixing ratio is, however, large. As can be seen from Fig. 10, all decays are consistent with a MS two-Q-phonon interpretation of the 3_2^+ state, to which we, therefore, assign MS character.

E. Possible 4^+ and 0^+ MS states?

Both the 4_2^+ and the 4_3^+ states show strong $M1$ decays to the 4_1^+ state. For the $4_2^+ \rightarrow 4_1^+$ transition, we determined a large $M1$ strength of $B(M1;4_2^+ \rightarrow 4_1^+) = 1.23(20)\ \mu_N^2$. This transition is the strongest $M1$ decay found in ^{94}Mo. The $4_2^+ \rightarrow 2_1^+$ $E2$ strength amounts to $B(E2;4_2^+ \rightarrow 2_1^+) = 5.9^{+1.0}_{-0.8}$ W.u., pointing to a rather collective transition. The combination of a strong $4_2^+ \rightarrow 4_1^+$ $M1$ transition and a collective $4_2^+ \rightarrow 2_1^+$ $E2$ transition falls out of the sd-IBM-2 scheme. Probably it is related to the excitation of g bosons in terms of the IBM. Indeed, recent calculations by Lisetskiy *et al.* [4] reproduce the $4_2^+ \rightarrow 4_1^+$ $M1$ transition strength in the spherical shell model with dominant components of seniority $\nu = 2$ in the 4_2^+ state's wave function pointing at g-boson character. This is discussed in Sec. IV G 2.

The 4_3^+ state at 2564.9 keV decays to the 4_1^+ state with a transition matrix element of $|\langle 4_1^+ \| M1 \| 4_3^+ \rangle| = 1.44(22)\mu_N$. We can, furthermore, give an upper limit for the $E2$ strength of $B(E2;4_3^+ \rightarrow 4_1^+) < 14.6$ W.u. Therefore, it is possible that the wave function of the 4_3^+ state contains components of a symmetric three-Q-phonon state with the structure $(2_1^+ \otimes 2_1^+ \otimes 2_1^+)^{4^+}$. However, a transition to the dominantly symmetric two-phonon 2_2^+ state was not observed. This contradicts a symmetric three-phonon interpretation. Instead, the $4_3^+ \rightarrow 2_1^+$ decay represents a weakly collective $E2$ transition with $B(E2;4_3^+ \rightarrow 2_1^+) = 1.1(3)$ W.u. Thus the 4_3^+ state is a candidate for a two-Q-phonon 4^+ MS state. But a decay to the 2_3^+ state, the $2^+_{1,\mathrm{ms}}$ state, was not identified. This may be a result of the low transition energy for an expected $4_3^+ \rightarrow 2_3^+$ decay. From the neutron scattering data, an upper limit for the $4_3^+ \rightarrow 2_3^+$ $E2$ strength of about 50 W.u. can be estimated, which leaves a collective $4_3^+ \rightarrow 2_3^+$ transition possible.

For another short-lived 4^+ state, the 4_4^+ state, the interpretation is unclear. Assuming a pure $M1$ decay, we determine an $M1$ transition strength of $B(M1;4_4^+ \rightarrow 4_1^+) = 0.090(11)\ \mu_N^2$, for pure $E2$ radiation an $E2$ strength of $B(E2;4_4^+ \rightarrow 4_1^+) = 36^{+5}_{-4}$ W.u. The decay to the 2_1^+ state has an $E2$ strength of $B(E2;4_4^+ \rightarrow 2_1^+) = 4.9^{+0.7}_{-0.5}$ W.u.

Besides the 0_3^+ state at 2780.5 keV, which will be discussed later in the context of symmetric three-Q-phonon excitations, no further 0^+ state was identified. Therefore, we have no information on the existence of a 0^+ MS state in ^{94}Mo.

F. Conclusion for two-Q-phonon MS states

As a conclusion, Fig. 9 shows the observed $M1$ transition strengths from the 2_2^+ state to the 1^+, 2^+, and 3^+ states in ^{94}Mo plotted versus the final level energy. Remark the nearly identical $M1$ transition strengths from the 2_2^+ state to the 1_2^+, 2_5^+, and 3_2^+ states and the closeness in excitation energy of these three states. No further excited states exhibit

TABLE II. Comparison of analytical IBM-2 predictions in the U(5) limit and in the O(6) limit with the core ^{100}Sn for $M1$ strengths of MS states with experimental data on ^{94}Mo. Orbital values, $g_\pi = 1\ \mu_N$ and $g_\nu = 0\ \mu_N$, are used for the boson g factors. All $M1$ strengths are given in μ_N^2.

Observable	U(5)	O(6)	Expt.
$B(M1;1^+_{\rm ms} \rightarrow 0^+_1)$	0	0.16	$0.160^{+0.011}_{-0.010}$
$B(M1;1^+_{\rm ms} \rightarrow 2^+_2)$	0.33	0.36	0.44(3)
$B(M1;2^+_{1,\rm ms} \rightarrow 2^+_1)$	0.23	0.30	0.56(5)
$B(M1;2^+_{2,\rm ms} \rightarrow 2^+_2)$	0.09	0.10	0.27(3)
$B(M1;3^+_{\rm ms} \rightarrow 4^+_1)$	0.12	0.13	0.075(10)
$B(M1;3^+_{\rm ms} \rightarrow 2^+_2)$	0.16	0.18	0.24(3)

the clear signatures of two-Q-phonon MS states, as dicussed before. Thus the 1^+_2, 2^+_5, and 3^+_2 states represent members of the two-Q-phonon multiplet of MS states with a moderately harmonic coupling because their excitation energies are close to the sum energy of the 2^+_1 and $2^+_{1,\rm ms}$ states of about 2940 keV.

G. Model calculations for MS states

1. IBM-2 predictions

It is natural to compare the data to the analytical predictions of the dynamical symmetry limits of the IBM. For the description of ^{94}Mo we consider the doubly closed-shell nucleus ^{100}Sn as the core and use $N_\pi = 4$ proton bosons and a single neutron boson. Due to the small number of valence neutrons, ^{94}Mo should be at most only weakly deformed excluding the SU(3) symmetry limit for reasonable comparison. The unusual low excitation energy of the 4^+_1 state with an $R_{4/2}$ value of only 1.81 indicates noncollective components in the 4^+_1 state. This $R_{4/2}$ value is somewhat below those expected for the U(5) limit ($R^{U(5)}_{4/2} = 2.0$) and the O(6) limit ($R^{O(6)}_{4/2} = 2.5$). A good destinction between the U(5) and O(6) limits is given by the K_4 value [64], which yields 1.0 in O(6) and 1.32 in U(5). The experimental value for ^{94}Mo is $K_4^{\rm approx.} = 1.14^{+0.18}_{-0.14}$ which is inconclusive on the symmetry character due to the large uncertainty. Therefore, we compare the data on electromagnetic transition strengths to both the U(5) and O(6) predictions.

We reduced the number of parameters in the $M1$ and $E2$ transition operators by restricting them to the proton parts alone:

$$T(M1) = \sqrt{3/4\pi} \cdot g_\pi L_\pi \tag{9}$$

$$T(E2) = e_\pi Q_\pi . \tag{10}$$

L_π and Q_π are the standard proton angular momentum operator and the proton quadrupole operator in the vibrational limit ($\chi_\pi = 0$), respectively. We accept the orbital value $g_\pi = 1\ \mu_N$ for the proton boson g factor, leaving the effective quadrupole boson charge $e_\pi = 9\ e\,{\rm fm}^2$ as the only adjustable parameter.

Table II compares some measured large $M1$ strengths to the IBM-2 predictions [65] in the U(5) and O(6) dynamical symmetry limits. The good agreement of most of the data with the predictions, both in the U(5) and O(6) dynamical symmetry limits, shows that these observables are not particulary sensitive to the symmetry character along the U(5)–O(6) transition. However, the $1^+_{\rm ms} \rightarrow 0^+_1$ transition found to be large experimentally cannot be described in the U(5) limit while it is well accounted for in the O(6) limit. In fact, by using the Ginocchio sum rule for the $M1$ strength [66] and the total $M1$ strength of $B(M1)\uparrow = 0.67(7)\ \mu_N^2$ observed below 4 MeV in ^{94}Mo one gets a ratio of 46(5)% d-bosons in the IBM-2 ground-state wave function. This large d-boson contribution to the ground-state wave function excludes ^{94}Mo as a pure U(5) nucleus, whereas the ground-state should contain 33% d-bosons in the O(6) limit. An analysis of the d-boson ratio of the ground state and the 2^+_2 state in a recent publication of Smirnova *et al.* [7] indicates ^{94}Mo to be a transitional nucleus between the O(6) and U(5) limits, but closer to the O(6) limit. The predictions from [65] are widely independent of Hamiltonian parameters and are simple analytical expressions, which involve the boson numbers and the parameters of the transition operators only.

The possible absence of a 0^+ two-Q-phonon MS state as stated above further supports the O(6) interpretation of ^{94}Mo, for which such a $0^+_{\rm ms}$ state is predicted to be missing from the two-Q-phonon multiplet [65]. On the other hand, a 0^+_2 state exists in ^{94}Mo at nearly exactly twice the excitation energy of the 2^+_1 state. This is not expected in the O(6) limit. But since there is no lifetime information for the 0^+_2 state because the only decay transition to the 2^+_1 state forms a doublet with the $2^+_1 \rightarrow 0^+_1$ transition, the structure of the 0^+_2 state is unclear, it could also be an intruder state outside of the sd-IBM-2 space.

Table III summarizes the experimental determined $M1$ and $E2$ transition strengths relevant for the identification of one- and two-Q-phonon MS states in ^{94}Mo in comparison to the predictions in the O(6) limit of the IBM-2 (third column). The qualitative agreement gives evidence for the MS interpretation of the 2^+_3, 1^+_2, 2^+_5, and 3^+_2 states.

2. Calculations in the spherical shell model and in the QPM

In recent publications the identified MS states in ^{94}Mo were studied microscopically within the spherical shell model [4] and in the quasiparticle-phonon model [5,6]. Both calculations are consistent with our experimental data and confirm the MS interpretation of these states from the IBM-2. The results of these calculations will be presented and we will compare them to our results.

Calculations in the spherical shell model [4] were done with the Hamiltonian $H = H_0 + V$, whereas H_0 represents the mean field Hamiltonian and V the residual surface delta interaction (SDI) [67]. ^{88}Sr was chosen as an inert core, considering four proton particles in the proton shells $\pi g_{9/2}$ and $\pi p_{1/2}$. Because of the Pauli principle, this problem is equivalent to the consideration of the doubly closed shell nucleus ^{100}Sn as an inert core with eight proton holes in the same shells.

TABLE III. Comparison of measured $M1$ and $E2$ transition strengths of the 2_3^+, 2_5^+, 3_2^+, and 1_2^+ states to predictions in the O(6) limit of the IBM-2 (third column) for the $2_{1,\mathrm{ms}}^+$, $2_{2,\mathrm{ms}}^+$, 3_{ms}^+, and 1_{ms}^+ states. Many transition strengths are reproduced on an absolute scale using a single free parameter, $e_\pi = 9\ e\,\mathrm{fm}^2$, only. $M1$ strengths are given in μ_N^2 and $E2$ strengths in W.u. In addition, columns 4 and 5 give the results of microscopic calculations for these states in the spherical shell model (SM) (from [4]) and in the QPM (from [5]). For $E2$ transitions the correlation between Weisskopf units and e^2 fm^4 is given by 1 W.u. $= 25.39\ e^2$ fm^4 for $A = 94$. If two values for the transition strengths are given, the multipole mixing ratio was ambiguous.

Observable	Expt.	IBM-2	SM	QPM
$B(M1;2_3^+ \to 2_1^+)$	0.56(5)	0.30	0.51	0.20
$B(M1;1_2^+ \to 0_1^+)$	$0.160^{+0.011}_{-0.010}$	0.16	0.26	0.08
$B(M1;1_2^+ \to 2_1^+)$	0.012(3)	0	0.002	0.003
$B(M1;1_2^+ \to 2_2^+)$	0.44(3)	0.36	0.46	0.42
$B(M1;1_2^+ \to 2_3^+)$	<0.05	0	0.08	0.003
$B(M1;2_5^+ \to 2_1^+)$	$0.0017^{+0.0010}_{-0.0012}$	0	0.004	0.008
$B(M1;2_5^+ \to 2_2^+)$	0.27(3)	0.100	0.17	0.56
$B(M1;2_5^+ \to 2_3^+)$	<0.16	0	0.06	
$B(M1;3_2^+ \to 2_1^+)$	$0.006^{+0.003}_{-0.004}$	0	0.10	0.004
$B(M1;3_2^+ \to 4_1^+)$	0.075(10)	0.13	0.058	0.12
$B(M1;3_2^+ \to 2_2^+)$	0.24(3)	0.18	0.09	0.17
$B(M1;3_2^+ \to 2_3^+)$	$0.021^{+0.016}_{-0.012}$	0	0.001	0.006
	0.09(2)			
$B(E2;0_1^+ \to 2_1^+)$	80(1)	91.9	82.7	81.4
$B(E2;0_1^+ \to 2_3^+)$	11.0(10)	5.9	8.27	3.94
$B(E2;0_1^+ \to 2_5^+)$	$0.70^{+0.09}_{-0.08}$	0	1.45	1.69
$B(E2;2_3^+ \to 2_1^+)$	$4.9^{+3.0}_{-2.3}$	0	0.001	0.039
$B(E2;1_2^+ \to 2_1^+)$	$0.72^{+0.27}_{-0.24}$	1.9	0.51	2.99
$B(E2;1_2^+ \to 2_2^+)$	$0.99^{+0.92}_{-0.62}$	0	0.055	0.35
$B(E2;1_2^+ \to 2_3^+)$	<27	21.9	8.98	29.1
$B(E2;2_5^+ \to 2_1^+)$	$0.40^{+0.19}_{-0.14}$	0.626	1.8	3.31
$B(E2;2_5^+ \to 2_2^+)$	$0.4^{+0.9}_{-0.4}$	0	1.2	
$B(E2;2_5^+ \to 2_3^+)$	<140	16.9	5.5	22.5
$B(E2;3_2^+ \to 2_1^+)$	$0.9^{+0.5}_{-0.4}$	1.90	1.70	2.76
$B(E2;3_2^+ \to 4_1^+)$	$0.14^{+0.30}_{-0.13}$	0	0.91	0.007
$B(E2;3_2^+ \to 2_2^+)$	$0.9^{+1.6}_{-0.8}$	0	6.70	0.35
$B(E2;3_2^+ \to 2_3^+)$	58(14)	14.6	7.81	25.4
	$9.5^{+12.5}_{-8.3}$			

The shell model calculations were performed using the code RITSSCHIL [68]. Both level energies and $M1$ and $E2$ transition strengths have been calculated, and reproduce the experimental data in most cases very well. For a comparison of the level energies, see [4]. The fourth column of Table III shows the shell model results of the $M1$ and $E2$ transition strengths for the observed MS states and the 2_1^+ state. The shell model calculations agree well with the IBM-2, with only a few exemptions. It should be mentioned that, for a good reproduction of the measured $M1$ strengths, pure isovector $M1$ transitions were used. Only for the 3_2^+ state do the transition strengths from the shell model disagree with the experimental data and the IBM-2. In fact, in the shell model calculation with the SDI and the ^{88}Sr core, the MS strength of the 3_{ms}^+ state turned out to be spread over the first three 3^+ states, which is an indication of the limit of this approach for states close in energy.

Finally, we want to stress that the strongest $M1$ transition observed in ^{94}Mo, the $4_2^+ \to 4_1^+$ $M1$ decay, cannot be described in the sd-IBM-2. A possible explanation for the 4_2^+ state is the interpretation as a one-phonon MS state resulting from a g-boson excitation, which then would be the first observation of a MS state in the g-boson sector, but further theoretical investigation in the IBM-2 is needed for a clear identification of this state in the IBM-2. On the other hand, the $4_2^+ \to 4_1^+$ $M1$ transition was reproduced in the shell model. The shell model result of $B_{\mathrm{SM}}(M1;4_2^+ \to 4_1^+) = 1.79\ \mu_N^2$ [4] is in good agreement with the experimental value.

The QPM calculations [5,6] were able to reproduce the MS character of the 2_3^+, 1_2^+, and 3_2^+ states. In the more recent publication [6], the agreement with the experimental data is even better than in the first one [5]. Lo Iudice and Stoyanov were able to reproduce both the excitation energies and the transition strengths for several low-lying states in ^{94}Mo in their microscopic calculations (for a comparison of the transition strengths, see Table III). The 2_3^+ state was predicted to have 95% of the structure of an isovector or MS one-phonon state. The calculated energy of 1940 keV matches rather well with the experimentally determined energy of 2067.4 keV. The 1_2^+ and 3_2^+ states were calculated to contain large two-phonon MS components of 90% and 87%, respectively, and good agreement of the excitation energies was achieved.

In addition, in the first publication [5], the wave function of the 2_5^+ state was predicted to contain 75% of the mixed-symmetry two-phonon 2^+ state, even before our recent publication identifying this state from measured $M1$ and $E2$ strengths [3]. The more recent calculation [6] predicted two 2^+ states at 2730 and 3014 keV with 27% and 59% MS two-phonon structures, respectively; i.e., in this case the MS two-phonon strength is predicted to be fragmented, which is not the case experimentally (see Fig. 9).

V. OTHER MULTIPHONON STATES

A. Symmetric two-quadrupole phonon states

Both the 2_2^+ and the 4_1^+ states show strong $E2$ decays to the 2_1^+ state. Using the lifetime from [57] for the 4_1^+ state, we get a collective transition strength of $B(E2;4_1^+ \to 2_1^+) = 26.0^{+4.2}_{-3.2}$ W.u., giving evidence that the 4_1^+ state contains large components of the symmetric two-Q-phonon 4^+ configuration. For the $2_2^+ \to 2_1^+$ transition we determine an $E2$ transition strength of $B(E2;2_2^+ \to 2_1^+) = 60^{+24}_{-31}$ W.u., which is in agreement with the interpretation of this state as a symmetric two-Q-phonon state.

It should be noted that the calculations in the QPM [5,6] reproduce the mainly symmetric two-phonon character of the 2_2^+ and 4_1^+ states. In the first publication [5] the 2_2^+ state is predicted to contain 77% of a symmetric two-phonon state, and the 4_1^+ state to contain 68%. The more recent calcula-

TABLE IV. Comparison of experimentally determined transition strengths of the 4_1^+ and the 2_2^+ states to the results of calculations with the IBM-2 in the dynamical O(6) symmetry, the spherical shell model (SM) [4], and the QPM [5,6]. $E2$ strengths are given in W.u. and $M1$ strengths in μ_N^2.

Observable	Expt.	IBM-2	SM	QPM [5]	QPM [6]
$B(E2;4_1^+\rightarrow 2_1^+)$	$26.0^{+4.2}_{-3.2}$	23.3	17.5	28.6	26.0
$B(E2;2_2^+\rightarrow 2_1^+)$	60^{+20}_{-30}	23.3	19.0	24.3	26.5
$B(M1;2_2^+\rightarrow 2_1^+)$	$0.026^{+0.041}_{-0.016}$	0	0.094	0.016	0.004
$B(E2;0_1^+\rightarrow 2_2^+)$	1.65(55)	0	2.17	0.83	1.38

tions [6] predict even higher symmetric two-phonon character for these states of 82% for both the 2_2^+ and the 4_1^+ state. The decay transition strengths of the 2_2^+ and 4_1^+ states were reproduced in the IBM-2, in the QPM [5,6], and in the spherical shell model [4] (see Table IV) supporting the mainly symmetric two-Q-phonon character. However, substantial components with seniority $\nu=2$ in the wave function of the 4_1^+ state calculated in the shell model indicate a more complicated structure.

Since the excitation energy of the 0_2^+ state is nearly exactly twice the energy of the 2_1^+ state and the only γ-ray decay is that to the 2_1^+ state, we did not get any information for this state from our data. No lifetime information is available for the 0_2^+ state from earlier measurements. The important question whether this state is a $\pi(p_{1/2})$ configuration or a collective two-phonon state cannot be answered by our data.

B. Symmetric three-quadrupole phonon states

Signatures for an expected quintuplet of symmetric three-Q-phonon excitations with the structure $(2_1^+\otimes 2_1^+\otimes 2_1^+)^{0^+,2^+,3^+,4^+,6^+}$ are collective $E2$ transitions to the symmetric two-Q-phonon states. The centroid of the three-Q-phonon multiplet should be at about three times $E(2_1^+)$ or 2.6 MeV. We now discuss candidates for members of this quintuplet identified from our data.

0^+ state. At 2780.5 keV the 0_3^+ state was identified. The transition strength of the only observed decay to the 2_2^+ state is $B(E2;0_3^+\rightarrow 2_2^+)=104^{+24}_{-21}$ W.u. Its excitation energy and the high collectivity of this decay gives evidence for this state being a symmetric three-Q-phonon 0^+ state. No further 0^+ states were identified in our measurements.

2^+ state. Besides the 2_3^+ and 2_5^+ states, identified as MS states, two additional 2^+ states below 3 MeV, the 2_4^+ state at 2393.1 keV and the 2_6^+ state at 2993.1 keV, were found. The 2_4^+ state shows a strong decay to the 2_1^+ state, but only a very weak decay to the 2_2^+ state, and thus is not a candidate for a symmetric three-Q-phonon state. The 2_6^+ state decays strongly to the 2_2^+ state with an $E2$ transition strength of $B(E2;2_6^+\rightarrow 2_2^+)=34.4^{+5.5}_{-4.9}$ W.u. A decay to the 2_1^+ state with dominant $E2$ character, but a transition strength of only $B(E2;2_6^+\rightarrow 2_1^+)=0.88(14)$ W.u. and a weak ground state decay were also observed. These observations indicate that the 2_6^+ state carries most of the symmetric three-Q-phonon strength. In addition, a rather strong $2_6^+\rightarrow 2_3^+$ $M1$ decay was observed with a transition strength of $B(M1;2_6^+\rightarrow 2_3^+)=0.068^{+0.011}_{-0.009}\,\mu_N^2$. This even supports the interpretation of the 2_6^+ state as a symmetric three-phonon state due to the d-parity selection rules [63]. These rules signify that $M1$ transitions are only allowed between states with the same d parity, i.e., $M1$ transitions do not change the number of quadrupole phonons, n_Q, modulo 2. Therefore, an $M1$ transition is to be expected for the decay transition from a three-Q-phonon state with the structure $(Q_sQ_sQ_s)^{2^+}|0_1^+\rangle$ and thus negative d parity to the one-Q-phonon $2_{1,\mathrm{ms}}^+$ state with the structure $Q_m|0_1^+\rangle$ and negative d parity. We want to stress that this is the first time the d-parity selection rules were confirmed in a decay transition from a symmetric multiphonon state *to* a MS state.

3^+ state. The 3_1^+ state at 2805.0 keV decays strongly to the 2_2^+ and 4_1^+ states with transition strengths of $B(E2;3_1^+\rightarrow 2_2^+)=19.0(39)$ W.u. and $B(E2;3_1^+\rightarrow 4_1^+)=9.2(15)$ W.u. A weak $3_1^+\rightarrow 2_1^+$ decay with an $E2$ transition strength of $B(E2;3_1^+\rightarrow 2_1^+)=0.74(11)$ W.u. under the assumption of pure $E2$ radiation was observed. From its decay characteristics, the 3_1^+ state can be identified as a clear candidate for a symmetric three-Q-phonon state.

4^+ state. Two 4^+ states around 2.6 MeV were observed but, because of the uncertainties of the $E2/M1$ mixing ratio of the $4_3^+\rightarrow 4_1^+$ decay and the unknown $E2/M1$ mixing ratio of the $4_4^+\rightarrow 4_1^+$ decay, no clear identification of these states as symmetric three-Q-phonon states was possible (see Sec. IV E). Transitions from neither of these states to the 2_2^+ state were observed.

6^+ state. The 6_1^+ state, a candidate for a symmetric three-phonon 6^+ state, was observed at 2423.4 keV. Only a lower limit for the lifetime of $\tau(6_1^+)>450$ fs was measured, which gives an upper limit for the $6_1^+\rightarrow 4_1^+$ $E2$ transition strength of $B(E2;6_1^+\rightarrow 4_1^+)<160$ W.u. Due to the possible collectivity of the $6_1^+\rightarrow 4_1^+$ decay and the fact that the 6_2^+ state at 2872.4 keV decays only to the 6_1^+ state and can therefore be excluded as a three-Q-phonon state, we interprete the 6_1^+ state as a candidate for the symmetric three-Q-phonon 6^+ state.

C. Quadrupole-octupole coupled structures

The coupling between the symmetric quadrupole phonon Q_s and the octupole phonon O produces a quintuplet of quadrupole-octupole coupled (QOC) states with the spin quantum numbers 1^-–5^- and the structure $(2_1^+\otimes 3_1^-)$ [14]. In a simple vibrational model with harmonic coupling this multiplet should lie at the sum energy of the 2_1^+ and 3_1^- states. In addition, for the 1^- member of the multiplet a rather strong $E1$ transition strength of the $1^-\rightarrow 0_1^+$ transition of the order of a milli Weisskopf unit is to be expected due to the collectivity. This $E1$ decay can be considerably stronger than other low-lying $E1$ transitions resulting, e.g., from single-particle transitions and should correlate to the $3_1^-\rightarrow 2_1^+$ $E1$ strength.

From the discussion above we have concluded that ^{94}Mo has a structure closer to the O(6) dynamical symmetry limit of the IBM rather than a pure vibrator. Weak coupling between the quadrupole and octupole degree of freedom leads similarly to a QOC two-phonon multiplet at the sum energy in O(6) [70]. Evidence for breaking of this weak coupling in γ-soft nuclei due to a residual quadrupole-quadrupole interaction comes from the study of octupole fragmentation [71]. Such a perturbation would lead to some anharmonicities for the QOC two-phonon multiplet.

A 1^- state was identified at 3260.8 keV in ^{94}Mo rather close to the sum energy of the 2_1^+ and the 3_1^- states of $E(2_1^+)+E(3_1^-)\approx 3400$ keV. The $E1$ transition strength to the ground state is $B(E1;1^-\rightarrow 0_1^+)=0.32^{+6}_{-4}\times 10^{-3}\ e^2\ \mathrm{fm}^2$. As was discussed in detail in [69], we expect from the naive phonon picture an $E1$ strength ratio of 7/3 for the $1^-\rightarrow 0_1^+$ and the $3_1^-\rightarrow 2_1^+$ transitions. From our measurements we obtained an $E1$ strength of $B(E1;3_1^-\rightarrow 2_1^+)=0.067^{+0.012}_{-0.010}\times 10^{-3}\ e^2\ \mathrm{fm}^2$, which is about a factor of 5 weaker than the $1^-\rightarrow 0_1^+$ transition. This disagreement may result from admixtures in the wave functions of these states, e.g., mixing of the 3_1^- and the 3_2^- states.

The 3_2^- state at 3011.5 keV represents a candidate for the QOC 3^- state. It lies about 400 keV below the sum energy of the 2_1^+ and 3_1^- state, but no additional 3^- states were identified. The decay transitions of the 3_2^- state give hints for this state having QOC character. For a QOC 3^- state, we expect the decay transitions to the symmetric two-Q-phonon 2_2^+ and 4_1^+ states to be about as strong as the $3_1^-\rightarrow 2_1^+$ and the $1_1^-\rightarrow 0_1^+$ decays, because the first two transitions should stem from the annihilation of a octupole phonon and the creation of a quadrupole phonon, the latter from the annihilation of both. $E1$ strengths of $B(E1;3_2^-\rightarrow 2_2^+)=0.071^{+0.019}_{-0.018}\times 10^{-3}\ e^2\ \mathrm{fm}^2$ and $B(E1;3_2^-\rightarrow 4_1^+)=0.115^{+0.028}_{-0.027}\times 10^{-3}\ e^2\ \mathrm{fm}^2$, respectively, were determined in our measurements. These values are comparable to the $3_1^-\rightarrow 2_1^+$ $E1$ strength. The $3_2^-\rightarrow 3_1^-$ decay should be a collective $E2$ transition with a transition strength comparable to the $2_1^+\rightarrow 0_1^+$ decay because both decays stem from the annihilation of the symmetric Q-phonon Q_s, if the 3_2^- is a QOC state. In fact, an upper limit for the $E2$ strength of $B(E2;3_2^-\rightarrow 3_1^-)<35$ W.u. was determined. On the other hand, the $3_2^-\rightarrow 3_1^-$ transition has a rather large $M1$ component of $B(M1;3_2^-\rightarrow 3_1^-)=0.39(7)\mu_N^2$, which could be a hint for MS components in the wave function of the 3_2^- state resulting from a MS f-boson excitation [70].

The 5_1^- state lies at 2610.5 keV. The $5_1^-\rightarrow 4_1^+$ decay transition strength amounts to $B(E1;5_1^-\rightarrow 4_1^+)=0.88(18)\times 10^{-3}\ e^2\ \mathrm{fm}^2$ which is one order of magnitude stronger than the $E1$ strength of the decay from the 3_1^- state to the 2_1^+ state. This and the low excitation energy about 800 keV lower than the sum energy of the 2_1^+ and 3_1^- states prevent this state from being interpreted as a clear candidate for a QOC state.

No candidates for the 2^- and 4^- members of the QOC quintuplet were found. Only a $J=(4^-)$ state at 2834.8 keV was identified, but the low excitation energy and the long lifetime of $\tau>1000$ fs are not in keeping with this state being a candidate for a QOC state.

VI. SUMMARY

Low-spin states in ^{94}Mo were investigated extensively using a combination of photon scattering experiments, a β-decay experiment, $\gamma\gamma$ coincidence studies with the reaction $^{91}\mathrm{Zr}(\alpha,n)^{94}\mathrm{Mo}$, and neutron scattering experiments. From our detailed data we were able to clearly identify the one-Q-phonon $2^+_{1,\mathrm{ms}}$ state and the 1^+, 2^+, and 3^+ members of the MS two-Q-phonon multiplet with the structure $(2_1^+\otimes 2^+_{1,\mathrm{ms}})$ from the measurement of absolute $M1$ and $E2$ transition strengths. Our interpretation of these states in the framework of the IBM-2 was supported by microscopic calculations in the spherical shell model [4] and the QPM [5,6]. Moreover, candidates for quadrupole-octupole coupled states and symmetric three-phonon states with the structure $(2_1^+\otimes 2_1^+\otimes 2_1^+)$ were found.

ACKNOWLEDGMENTS

We thank A. Fitzler, C. Friessner, I. Schneider, and H. Tiesler for help with the experiments. We acknowledge discussions with A. Gelberg, F. Iachello, N. Lo Iudice, T. Otsuka, Ch. Stoyanov, I. Wiedenhöver, and R. F. Casten. This work was supported by the Deutsche Forschungsgemeinschaft under Contract Nos. Br 799/8-2/9-1, Kn 154/30, and Pi 393/1-1/1-2, and by the U.S. National Science Foundation under Grant No. PHY-0098813.

[1] N. Pietralla, C. Fransen, D. Belic, P. von Brentano, C. Friessner, U. Kneissl, A. Linnemann, A. Nord, H.H. Pitz, T. Otsuka, I. Schneider, V. Werner, and I. Wiedenhöver, Phys. Rev. Lett. **83**, 1303 (1999).

[2] N. Pietralla, C. Fransen, P. von Brentano, A. Dewald, A. Fitzler, C. Friessner, and J. Gableske, Phys. Rev. Lett. **84**, 3775 (2000).

[3] C. Fransen, N. Pietralla, P. von Brentano, A. Dewald, J. Gableske, A. Gade, A. Lisetskiy, and V. Werner, Phys. Lett. B **508**, 219 (2001).

[4] A. Lisetskiy, N. Pietralla, C. Fransen, R.V. Jolos, and P. von Brentano, Nucl. Phys. **A677**, 100 (2000).

[5] N. Lo Iudice and Ch. Stoyanov, Phys. Rev. C **62**, 047302 (2000).

[6] N. Lo Iudice and Ch. Stoyanov, Phys. Rev. C **65**, 064304 (2002).

[7] N.A. Smirnova, N. Pietralla, A. Leviatan, J.N. Ginocchio, and C. Fransen, Phys. Rev. C **65**, 024319 (2002).

[8] N. Pietralla, C.J. Barton, III, R. Krücken, C.W. Beausang, M.A. Caprio, R.F. Casten, J.R. Cooper, A.A. Hecht, H. Newman, J.R. Novak, and N.V. Zamfir, Phys. Rev. C **64**, 031301(R) (2001).

[9] H. Klein, A.F. Lisetskiy, N. Pietralla, C. Fransen, A. Gade, and P. von Brentano, Phys. Rev. C **65**, 044315 (2002).
[10] A. Bohr and B.R. Mottelson, *Nuclear Structure* (Benjamin, New York, 1975), Vol. 2.
[11] F. Corminboeuf, T.B. Brown, L. Genilloud, C.D. Hannant, J. Jolie, J. Kern, N. Warr, and S.W. Yates, Phys. Rev. Lett. **84**, 4060 (2000).
[12] P. Kleinheinz, J. Styczen, M. Piiparinen, J. Blomqvist, and M. Kortelahti, Phys. Rev. Lett. **48**, 1457 (1982).
[13] N. Pietralla, in *LEPS2000*, edited by M. Yosoi and H. Shimizu (RCNP, Osaka University, 2000), p. 97.
[14] P.O. Lipas, Nucl. Phys. **82**, 91 (1966).
[15] C. Fransen, O. Beck, P. von Brentano, T. Eckert, R.-D. Herzberg, U. Kneissl, H. Maser, A. Nord, N. Pietralla, H.H. Pitz, and A. Zilges, Phys. Rev. C **57**, 129 (1998).
[16] W. Andrejtscheff, C. Kohstall, P. von Brentano, C. Fransen, U. Kneissl, and N. Pietralla, and H.H. Pitz, Phys. Lett. B **506**, 239 (2001).
[17] A. Arima, T. Otsuka, F. Iachello, and I. Talmi, Phys. Lett. **66B**, 205 (1977).
[18] T. Otsuka, Boson Model of Medium-Heavy Nuclei, Ph.D. thesis, University of Tokyo, 1978; F. Iachello, Lecture Notes on Theoretical Physics, Groningen, 1976.
[19] T. Otsuka, A. Arima, and F. Iachello, Nucl. Phys. **A309**, 1 (1978).
[20] F. Iachello, Phys. Rev. Lett. **53**, 1427 (1984).
[21] P. van Isacker, K. Heyde, J. Jolie, and A. Sevrin, Ann. Phys. (N.Y.) **171**, 253 (1986).
[22] A. Faessler, Nucl. Phys. **85**, 653 (1966).
[23] G. Siems, U. Neuneyer, I. Wiedenhöver, S. Albers, M. Eschenauer, R. Wirowski, A. Gelberg, P. von Brentano, and T. Otsuka, Phys. Lett. B **320**, 1 (1994).
[24] T. Otsuka and K.H. Kim, Phys. Rev. C **50**, R1768 (1994).
[25] N. Pietralla, T. Mizusaki, P. von Brentano, R.V. Jolos, T. Otsuka, and V. Werner, Phys. Rev. C **57**, 150 (1998).
[26] N. Pietralla, P. von Brentano, R.-D. Herzberg, U. Kneissl, N. Lo Iudice, H. Maser, H.H. Pitz, and A. Zilges, Phys. Rev. C **58**, 184 (1998).
[27] K.H. Kim, T. Otsuka, P. von Brentano, A. Gelberg, P. van Isacker, and R.F. Casten, in *Capture Gamma-Ray Spectroscopy and Related Topics*, edited by G. Molnár (Springer, Budapest, 1996), Vol. I, p. 195.
[28] N. Pietralla, D. Belic, P. von Brentano, C. Fransen, R.-D. Herzberg, U. Kneissl, H. Maser, P. Matschinsky, A. Nord, T. Otsuka, H.H. Pitz, V. Werner, and I. Wiedenhöver, Phys. Rev. C **58**, 796 (1998).
[29] P.E. Garrett, H. Lehmann, C.A. McGrath, M. Yeh, and S.W. Yates, Phys. Rev. C **54**, 2259 (1996).
[30] R. De Leo, H. Akimune, N. Blasi, I. Daito, Y. Fujita, M. Fujiwara, S.I. Hayakawa, S. Hatori, K. Hosono, H. Ikegami, T. Inomata, I. Katayama, K. Katori, L. Lagamba, S. Micheletti, S. Morinobu, T. Nakagawa, S. Nakayama, A. Narita, T. Noro, R. Perrino, M. Pignanelli, H. Sakaguchi, J. Takamatsu, A. Tamii, K. Tamura, M. Tanaka, A. Terakawa, T. Tohei, M. Tosaki, T. Yamagata, A. Yamagoshi, M. Yosimura, and M. Yosoi, Phys. Rev. C **53**, 2718 (1996).
[31] W.D. Hamilton, A. Irbäck, and J.P. Elliott, Phys. Rev. Lett. **53**, 2469 (1984).
[32] G. Molnár, R.A. Gatenby, and S.W. Yates, Phys. Rev. C **37**, 898 (1988).
[33] N. Lo Iudice and F. Palumbo, Phys. Rev. Lett. **41**, 1532 (1978).
[34] D. Bohle, A. Richter, W. Steffen, A. Dieperink, N. Lo Iudice, F. Palumbo, and O. Scholten, Phys. Lett. **137B**, 27 (1984).
[35] A. Richter, Prog. Part. Nucl. Phys. **34**, 261 (1995).
[36] U. Kneissl, H.H. Pitz, and A. Zilges, Prog. Part. Nucl. Phys. **37**, 349 (1996).
[37] N. Pietralla, P. von Brentano, R.-D. Herzberg, U. Kneissl, J. Margraf, H. Maser, H.H. Pitz, and A. Zilges, Phys. Rev. C **52**, R2317 (1995).
[38] P. von Neumann-Cosel, J.N. Ginocchio, H. Bauer, and A. Richter, Phys. Rev. Lett. **75**, 4178 (1995).
[39] J. Enders, H. Kaiser, P. von Neumann-Cosel, C. Rangacharyulu, and A. Richter, Phys. Rev. C **59**, R1851 (1999).
[40] J.R. Vanhoy, J.M. Anthony, B.M. Haas, B.H. Benedict, B.T. Meehan, S.F. Hicks, C.M. Davoren, and C.L. Lundstedt, Phys. Rev. C **52**, 2387 (1995).
[41] S.F. Hicks, C.M. Davoren, W.M. Faulkner, and J.R. Vanhoy, Phys. Rev. C **57**, 2264 (1998).
[42] A. Giannatiempo, A. Nannini, and P. Sona, Phys. Rev. C **58**, 3316 (1998); **58**, 3335 (1998).
[43] P. Petkov, J. Gableske, O. Vogel, A. Dewald, P. von Brentano, R. Krücken, R. Peusquens, N. Nicolay, A. Gizon, J. Gizon, D. Bazzacco, C. Rossi-Alvarez, S. Lunardi, P. Pavan, D.R. Napoli, W. Andrejtscheff, and R.V. Jolos, Nucl. Phys. **A640**, 293 (1998).
[44] N. Pietralla, I. Bauske, O. Beck, P. von Brentano, W. Geiger, R.-D. Herzberg, U. Kneissl, J. Margraf, H. Maser, H.H. Pitz, and A. Zilges, Phys. Rev. C **51**, 1021 (1995).
[45] J. K. Tuli, Nucl. Data Sheets **66**, 1 (1992).
[46] Program code CASCADE, F. Pühlhofer, Nucl. Phys. **A270**, 267 (1977).
[47] J. Eberth, Prog. Part. Nucl. Phys. **28**, 495 (1992).
[48] G. Winter, Nucl. Instrum. Methods Phys. Res. **214**, 537 (1983).
[49] L.C. Northcliffe and R.F. Schilling, Nucl. Data, Sect. A **7**, 233 (1970).
[50] Y. Sugiyama and S. Kikuchi, Nucl. Phys. **A264**, 179 (1976).
[51] M.T. McEllistrem, J.D. Brandenberger, K. Sinram, G.P. Glasgow, and K.C. Chung, Phys. Rev. C **9**, 670 (1974).
[52] B. Fazekas, T. Belgya, G. Molnár, Á. Veres, R.A. Gatenby, S.W. Yates, and T. Otsuka, Nucl. Phys. **A548**, 249 (1992), and references therein.
[53] K.B. Winterbon, Nucl. Phys. **A246**, 293 (1975).
[54] K.B. Winterbon, Atomic Energy of Canada Limited Report No. AECL-4829.
[55] R.B. Firestone, in *Table of Isotopes*, 8th ed., edited by V.S. Shirley (Wiley Interscience, New York, 1996).
[56] E. Sheldon and V. C. Rogers, Comput. Phys. Commun. **6**, 99 (1973).
[57] J.K. Tuli, Nucl. Data Sheets **66**, 1 (1992); updated by M.R. Bhat (1997).
[58] E. Adamides, L.D. Skouras, and A.C. Xenoulis, Phys. Rev. C **23**, 2016 (1981).
[59] J.E. Holden and W.W. Daehnick, Phys. Rev. C **8**, 2286 (1973).
[60] E. Fretwurst, G. Lindstrom, K.F. von Regen, V. Riech, S.I. Vasilijev, P.P. Zarubin, O.M. Knyazkov, and I.N. Kukhtina, Nucl. Phys. **A468**, 247 (1987).
[61] E.R. Flynn, F. Ajzenberg-Selove, R.E. Brown, J.A. Cizewski,

and J.W. Sunier, Phys. Rev. C **24**, 2475 (1981).
[62] M. Pignanelli, N. Blasi, S. Micheletti, R. De Leo, L. La Gamba, R. Perrino, J.A. Bordewijk, M.A. Hofstee, J.M. Schippers, S.Y. van der Werf, J. Wesseling, and M.N. Harakeh, Nucl. Phys. **A540**, 27 (1992).
[63] N. Pietralla, P. von Brentano, A. Gelberg, T. Otsuka, A. Richter, N. Smirnova, and I. Wiedenhöver, Phys. Rev. C **58**, 191 (1998).
[64] V. Werner, N. Pietralla, P. von Brentano, R.F. Casten, and R.V. Jolos, Phys. Rev. C **61**, 021301(R) (2000).
[65] P. van Isacker, K. Heyde, J. Jolie, and A. Sevrin, Ann. Phys. (N.Y.) **171**, 253 (1986).
[66] J.N. Ginocchio, Phys. Lett. B **265**, 6 (1991).
[67] A. Plastino, R. Arvieu, and S.A. Moszkowski, Phys. Rev. **145**, 837 (1966).
[68] D. Zwarts, Comput. Phys. Commun. **38**, 365 (1985).
[69] N. Pietralla, Phys. Rev. C **59**, 2941 (1999).
[70] N.A. Smirnova, N. Pietralla, T. Mizusaki, and P. van Isacker, Nucl. Phys. **A678**, 235 (2000).
[71] N.V. Zamfir, P.D. Cottle, J.L. Johnson, and R.F. Casten, Phys. Rev. C **48**, 1745 (1993).